June 2025

Impact of Polycystic Ovarian Condition upon PGK1 Expression and Glucose Uptake in Granulosa Cells

Project report submitted to Sister Nivedita University in partial fulfillment of the requirement for the degree of

MASTER OF SCIENCE IN BIOTECHNOLOGY

Submitted by

SHREYASI KARMAKAR

REGISTRATION No.: 230020071178

Enrollment ID: 2322210002007

SESSION: 2023-2025

Under the guidance of

DR. PARAMITA SAHA

Assistant Professor

School of Health Science and Translational Research

Sister Nivedita University

PRESIDENCY UNIVERSITY
KOLKATA

Presidency University

Hindoo College (1817-1855), Presidency College (1855-2010)

CERTIFICATE

This is to certify that the dissertation work entitled **"Impact of Polycystic Ovarian Condition upon PGK-1 Expression and Glucose Uptake in Granulosa Cells"** has been submitted by **Ms. Shreyasi Karmakar** enrolled at Sister Nivedita University, ERN# 2322210002007 and Registration # 230020071178. The work is an original research work done by her under my supervision at **Institute of Health Sciences, Presidency University**; during the fourth semester of academic year 2024-2025 for the partial fulfillment of Master of Science degree in Biotechnology from Sister Nivedita University, Kolkata.

Paramita Saha

Dated: 21/05/2025

(Name and Signature of Supervisor
With Stamp)

Dr. Paramita Saha, Ph.D
Assistant Professor
Institute of Health Sciences
Presidency University (2nd Campus)
New Town, Kolkata-700156

86/1, College Street, Kolkata - 700073, Phone: (033) 2241 1960, Fax: (033) 2241 2738

DECLARATION BY STUDENT

I hereby declare that the work which is being presented in this dissertation entitled **"Impact of Polycystic Ovarian Condition upon PGK1 Expression and Glucose Uptake in Granulosa Cells"** in partial fulfillment of the requirements for the award of the degree of Masters of Science in Biotechnology, is an authentic record of my own work carried out during the period from January to March under the supervision of Dr. Paramita Saha, Department of 'Institute of Health Science', Presidency University.

I acknowledge that I have read and understood the UGC regulations, 2018 (Promotion of Academic integrity and Prevention of Plagiarism in Higher Educational Institutions).

I confirm that this dissertation has been checked for plagiarism using the plagiarism checking software 'Check Plagiarism Online'. At the end of the dissertation, a copy of the summary report demonstrating similarities in content and its potential source, generated online using plagiarism checking software is enclosed. I herewith confirm that the dissertation has been less than 10% similarity according to the plagiarism checking software's report and meets the UGC Regulations as well as plagiarism rules of Sister Nivedita University.

I further declare that no portion of dissertation or its data will be published without the Institute's or supervisor's permission. I have not previously applied for any other degree or award using the topics and findings described in my dissertations.

Shreyasi Karmakar
(5.6.2025)

(Signature of the student with date)

Name of the student: Shreyasi Karmakar

Registration No.: 230020071178

Department: Biotechnology

SISTER NIVEDITA UNIVERSITY
সিস্টার নিবেদিতা বিশ্ববিদ্যালয়

DG Block - 1/2, Action Area I, New Town, Kolkata - 700156, West Bengal, India.

DEPARTMENT OF BIOTECHNOLOGY & DEPARTMENT OF MICROBIOLOGY
জৈব প্রযুক্তি বিভাগ ও অণুজীব বিদ্যা বিভাগ

TO WHOM IT MAY CONCERN

This is to certify that the project report titled "**Impact of Polycystic Ovarian Condition upon PGK1 Expression and Glucose Uptake in Granulosa Cells**", submitted by Ms. Shreyasi Karmakar (Registration No.: 230020071178, Enrolment No.: 2322210002007) to the Department of Biotechnology, School of Health Science and Translational Research at Sister Nivedita University, Kolkata, is a bona fide record of research conducted by her for the partial fulfillment of the requirements for the Master of Science degree.

Date: 03.06.2025.

Place: SISTER NIVEDITA UNIVERSITY

Signature of Head of the Department

Seal

Head
Department of Biotechnology
Sister Nivedita University
Block DG-1/2, Action Area 1
New Town, Kolkata-700 156

ACKNOWLEDGEMENT

I would like to express my sincere gratitude to, ***Dr. Paramita Saha,*** *Assistant Professor, Presidency University, Kolkata, for giving me this opportunity to grow my expertise on different experimental techniques related to this dissertation project. It was a great experience for me to learn and developed professional skills to flourish in near future. Therefore, I hold myself to be fortunate enough to be a part of her lab. I am extremely grateful to my mentor for the constant support, valuable advices, motivation & encouragement which I received throughout this dissertation period, without which it would have been impossible for me to complete this project within this stipulated time. I am also equally grateful enough to those people whom I met and worked with during this course of internship. Specially, I would like to thank my lab seniors* ***Ms. Abhipsha Ray****,* ***Ms. Ruksana Parvin Ansary*** *and* ***Mr. Pritam Chowdhury*** *for their constant support that led me through this project. The way they helped me in each and every step of this project is truly praiseworthy. It was a wonderful time spent with them and these memories will stay evergreen for the rest of my life. I express my heartfelt gratitude to these people for taking part in right decisions, providing me with necessary advices and arranging for the facilities to make my work easier.*

I would also like to express my sincere gratitude to the neighbouring labs of ***Dr. Somsubhra Nath****,* ***Dr. Junaid Jibran Jawed****,* ***Dr. Debanjan Mukhopadhyay*** *and* ***Dr. Abhik Saha****, Assistant Professors of Institute of Health Sciences, Presidency University, Kolkata for extending the all- time cooperation with the lab consumables & instruments of them. Even this project claims special thanks to Google & PubMed for furnishing me with all-round information and the best updates associated with this piece of project.*

Last but not the least, my heartfelt gratitude to my special ones, my parents for their immense support which I received throughout my academic career without whom I could not have put a single step forward.

I perceive this opportunity as a big milestone to my further career development and will strive to use this gained knowledge in every possible way to do something better that will benefit this society. I will try to keep my quest for knowledge this way in order to achieve my desired career objectives. Thanks to all of you for this kind of cooperation.

Sincerely,

Name: Shreyasi Karmakar

MSc. in Biotechnology, Semester IV

Registration No.: 230020071178

School of Health Sciences and Translational Research,

Sister Nivedita University

LIST OF FIGURES

S. No.	Title
Figure 1	Interplay between granulosa cells and oocyte.
Figure 4.2A	Generation of different experimental sets (Control, Super-ovulated, PCO-induced and TQ pre-treated) utilizing KK-1 cell line.
Figure 4.2B	Flowchart of cDNA preparation protocol
Figure 4.2C	BSA standard Graph obtained from BSA known Concentration.
Figure 4.2D	Image showing the working principle of 2-NBDG.
Figure 5.1	Differential expression of glycolytic enzymes GAPDH and PGK1 under PCO condition
Figure 5.2	Predicted interaction between AR and PGK1 from bioinformatics analysis
Figure 5.3	Modulation of PGK1 expression by DHT and AR blocker Enzalutamide
Figure 5.4	Immunofluorescence analysis shows nuclear co-localization of AR and PGK1 in PCO samples
Figure 5.5A & 5.5B	GLUT-4 expression is upregulated in PCO samples in comparison to SO samples and this augmentation is reverted back by TQ treatment.
Figure 5.5C	Subcellular localization of GLUT-4 in the various experimental sets.
Figure 5.6	Analysis of 2-NBDG uptake in GCs through fluorescence microscopy
Figure 6	Flowchart describing the mechanism of impaired folliculogenesis and ovulation caused by PGK1 overexpression

LIST OF TABLES

S. No.	Title
Table 1	Nanodrop readings for RNA concentration, $A_{260/280}$ reading and volume (µl) required for 1 µg of RNA from ovary samples to be used for cDNA preparation.
Table 2	The exact volume of reagents for cDNA preparation reaction.
Table 3	Primer sequences of genes for amplification.

ABBREVIATIONS

S. No.	Abbreviations used	Extensions
1	PCOS	Polycystic Ovary Syndrome
2	IR	Insulin Resistance
3	GC	Granulosa Cell
4	AR	Androgen Receptor
5	KK-1	Murine Granulosa Cell Line
6	PGK1	Phosphoglycerate kinase-1
7	GLUT	Glucose transporter
8	PBS	Phosphate Buffered Saline
9	PBST	Phosphate Buffered Saline with 0.05% Tween-20
10	RT	Room Temperature
11	RIPA	Radio-immunoprecipitation Assay
12	BSA	Bovine Serum Albumin
13	SDS	Sodium Dodecyl Sulphate
14	TEMED	Tetramethylethylenediamine
15	APS	Ammonium Persulfate
16	HRP	Horseradish Peroxidase
17	hCG	Human Chorionic Gonadotropin
18	TQ	Thymoquinone
19	NFW	Nuclease Free Water
20	ROS	Reactive Oxygen Species

ABSTRACT: -

Polycystic ovary syndrome (PCOS) is a multifactorial disorder characterized by hyperandrogenism, anovulation/oligo-ovulation and insulin resistance (IR). Elevated expression of the androgen receptor (AR) under PCO condition has both reproductive as well as metabolic implications. AR situationally associates with glycolytic factors like insulin like growth factor-1 (IGF-1) and phospho-glycerate kinase 1 (PGK1), leading to differential glycolysis. The granulosa cells (GCs), which surround the developing ovum are involved in a delicate play of hormones, which is dysregulated in PCOS. Utilizing an established *in-vitro* PCOS model comprising of mouse granulosa cell line, KK-1; our study showed that the glycolytic enzyme GAPDH was significantly downregulated while PGK1 was significantly upregulated at both the transcript and protein levels in the PCO set in comparison to the super-ovulated (SO) controls. Potential interaction between AR and PGK1 was also predicted using *in silico* tools, signifying AR's role in elevating PGK1 expression under PCOS. PGK1 expression was also found to be upregulated in DHT treated KK-1 cells and was reversed upon treatment with AR-blocker enzalutamide; signifying AR activation is a driving force towards upregulation of PGK1. Furthermore, immunofluorescence studies confirmed elevated expression and nuclear localization of AR and PGK1 under PCO condition. Along with that, our study showed that under PCOS condition, significant upregulation of GLUT-4 leads to increased glucose uptake in GCs and it was also demonstrated that those abnormalities seen under PCOS is reversed upon thymoquinone (TQ) treatment, thus highlighting its therapeutic potential.

Keywords: - PCOS, PGK1, GLUTs, Granulosa cells, Androgen receptor, Insulin Resistance, Glucose uptake.

CONTENTS

S.NO.	TOPICS	PAGE NO.
1	Introduction	10
2	Review of Literature	12
3	Aims & Objectives	16
4	Materials and Methods	
	4.1 Materials	17
	4.2 Methods	18
	4.2.1 Mammalian cell culture	18
	4.2.2 RNA extraction, estimation & purity checking	20
	4.2.3 cDNA preparation and gene amplification by qPCR	21
	4.2.4 Protein sample preparation from experimental set cell lysates and concentration estimation	22
	4.2.5 Sodium Dodecyl Sulfate Polyacrylamide Gel Electrophoresis	24
	4.2.6 Western Blotting	24
	4.2.7 Detection of protein by enhanced chemiluminescence (ECL) or colorimetry	24
	4.2.8 Immunofluorescence studies	25
	4.2.9 Glucose uptake assay using 2-NBDG	26
	4.2.10 Statistical analysis	27
5	Results & Discussions	27
6	Conclusion	35
7	References	36
8	Plagiarism Report	38

1. INTRODUCTION

Polycystic ovary syndrome (PCOS) is a common endocrine disorder and gynecological ailment [1] characterized by impaired folliculogenesis and ovulatory dysfunction [2]. It is also one of the primary causes of infertility among females [3]. Women diagnosed with PCOS often experiences various metabolic or endocrine disruptions in which the primary defining features of PCOS are irregular menstruation, insulin resistance and hyperandrogenism respectively [2].

Insulin resistance (IR), a major symptom of PCOS, refers to a state where body cells do not uptake glucose properly and results in hyperinsulinemia and type 2 diabetes [4]. IR and hyperinsulinemia can play significant role in PCOS pathogenesis by interacting with other inflammatory biomarkers [5]. Also increase in insulin level in IR condition may increase the level of IGF-1 and their interaction with IGF-1 receptor has been shown to inhibit AR repressor (FOXO1) causing an upregulated AR transcription, which further worsens the PCOS condition causing hyperandrogenism [6].

Hyperandrogenism is a key hormonal imbalance that also gives rise to other PCOS symptoms like acne [6] and androgenic alopecia. Under normal physiological condition, LH stimulates the theca cells to produce androgens which is converted to estrogens by CYP19A1 (aromatase) enzyme expressed by GCs [7]. Increased expression of CYP19A1 implies normal pre-ovulatory follicles but researchers have shown that in PCO condition, CYP19A1 enzyme expression and level of estradiol was strikingly downregulated than normal follicles [8 9]. The hyperandrogenism in PCOS occurs due to low levels of aromatase that results into higher level of androgens and androgen receptor (AR). Previous studies demonstrated the upregulation of AR under polycystic ovarian condition using both *in vitro* and *in vivo* models [8].

In the ovaries, the process of folliculogenesis, which refers to the development of ovarian follicles into mature oocyte, along with the generation of functional granulosa cells (GCs), is tightly regulated under the influence of FSH and hypothalamic-pituitary-ovarian axis. Proper occurrence of folliculogenesis involves two-way interaction and coordination between GCs and oocytes. GCs, situated surrounding the oocyte, are the essential elements that contribute to the healthy ovarian physiology by controlling the complex system of hormonal regulation and providing appropriate environment for follicular maturation [10]. The development and maturation of oocyte requires excess amount of energy which is primarily fueled by glucose through glycolytic pathway, the most widely available energy

substrate in the body [11]. GCs uptake large amount of glucose with the help of glucose transporter proteins (GLUTs) on their surface, and produce glycolytic metabolites such as pyruvate and lactate because of high enzymatic activity followed by supplying pyruvate and lactate to the oocyte which is not efficient in conducting glycolysis due to the lack of glucose transporter proteins (GLUTs) on their surface and glycolytic enzymes [10]. This phenomenon is mediated by pyruvate dehydrogenase kinase (PDK) expressed by cumulus GCs that inhibits pyruvate dehydrogenase (PDH) and prevents the entry of pyruvate in TCA cycle within GCs [10]. The GCs thus fulfills the energy needs of the oocyte through generation of increased levels of pyruvate and lactate (**Figure 1**).

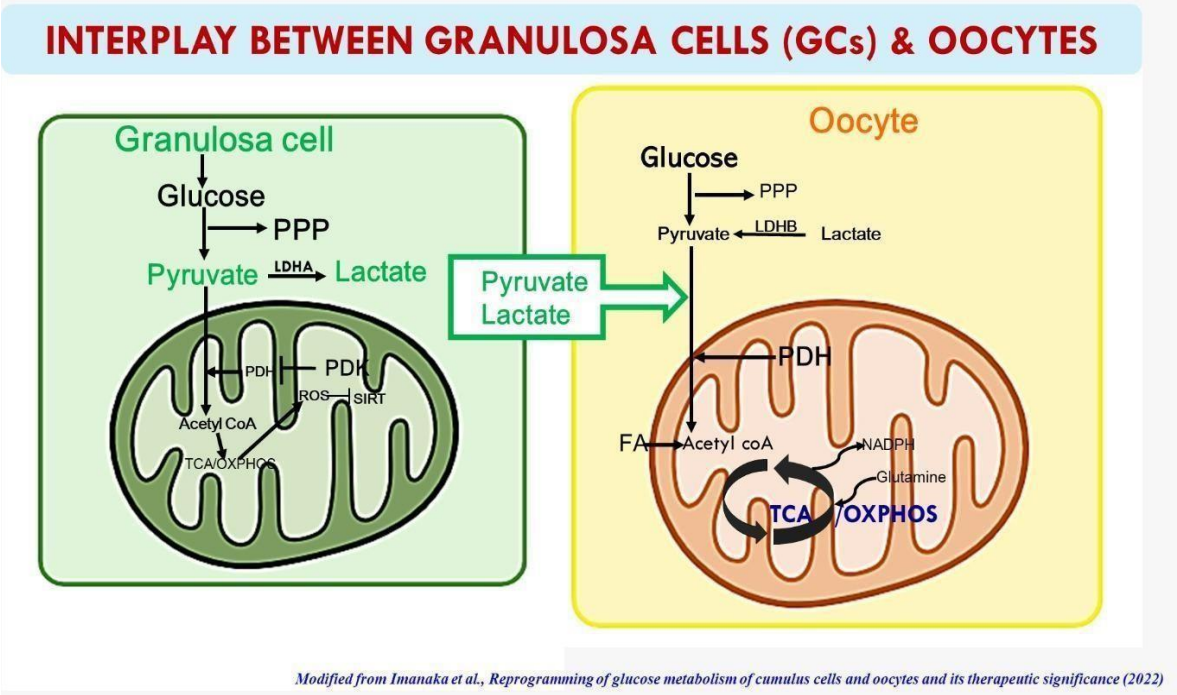

Figure 1: Interplay between granulosa cells and oocyte.

GLUTs are specialized kind of proteins present on the surface of GCs that assists in effective glucose transportations across cell membrane [11]. Among various types of GLUTs, GLUT-1 is constitutively expressed while GLUT-4 is differentially expressed [11]. Under normal physiology, GLUT-1 is primarily present on the surface of GCs. But in PCOS condition owing to insulin resistance, GLUT-4 is upregulated and GLUT-1 is downregulated in human GCs [11]. Efficient glycolysis for supporting folliculogenesis relies heavily on two important enzymes namely glyceraldehyde-3-phosphate dehydrogenase (GAPDH) and phosphoglycerate kinase-1 (PGK1) [12 13]. GAPDH catalyzes the sixth step in glycolysis by converting glyceraldehyde-3-phosphate (GAP) into 1,3-bisphosphoglycerate (1,3-bisPG) in the presence of NAD^+ and inorganic phosphate, which is the first redox

reaction of glycolysis [12] and also PGK1 catalyzes the first ATP producing step of glycolysis by converting 1,3-bisPG into 3-phophoglycerate. PGK1 plays important role in driving the glycolytic pathway forward in GCs and thus optimally supplying energy for proper folliculogenesis [11]. It is hypothesized that PGK1 might have positive correlation with AR [13]. PGK1 is thought to interact with AR present in GCs [14]. Another study has demonstrated that in the luteinized GCs of PCOS patients and ovarian tissues of PCOS like mouse models, PGK1 level is increased which further exacerbates the PCOS like symptoms in mouse models. However, the exact mechanism through which PGK1 controls the glucose metabolism in GCs and contributes to IR and other metabolic disorders, is still unclear [14]. Apart from this, differential expression of GLUTs and glycolytic enzymes has been observed in endometrial tissues of PCOS patients [15] but there are no studies about expression profiles of the GLUTs and glycolytic enzymes in local ovarian tissues and GCs.

Since there are various studies about differential expressions of glycolytic enzymes and GLUTs only in endometrial tissues, the present study intends to inspect if there are alterations of the same at the local ovarian tissues. This study utilizes already established *in vitro* PCOS models which were generated using murine GC line, named KK-1. Several studies have been performed using KK-1 as a model. This cell line is an excellent system for studies because it exhibits the characteristics of a typical GC, e.g. responsiveness to gonadotropins and inhibin expression. In addition, KK-1 cells can be easily maintained in culture and transfected with high efficiency. Studies on the RU486 treated hormone primed ovarian granulosa cell line KK-1, displayed some molecular features similar to what is observed in GCs from PCOS patients [8].

2. REVIEW OF LITERATURE

During the active reproductive years in women, a recurring pattern of hormonal shifts occurs each month, bringing about a sequence of functional changes in the ovaries and other reproductive organs. This regular biological rhythm, driven by the rise and fall of female sex hormones, governs the preparation for potential fertility and is formally recognized as the female monthly reproductive cycle, commonly known as the menstrual cycle [16]. The process consists of strict hormonal control which is regulated by hypothalamus. The hypothalamus produces GnRH hormone which stimulates anterior pituitary gland to secrete two important gonadotropins - FSH (follicle stimulating hormone)

and LH (luteinizing hormone). FSH and LH stimulate the growth and development of Graafian follicles in ovary and leads to ovulation and estrogen production.

The growth of follicles from the primordial follicles to primary oocytes via formation of oogonial mother cell (2n) in human embryonic ovaries takes approx. 6.5 months. During the last 2 weeks, formation of antral follicles occurs which is characterized by slower oocyte growth, extracellular fluid formation, granulosa cell (GCs) differentiation into mural and cumulus phenotypes, and selection of a dominant follicle. Early antral follicles in human are under the influence of and are highly responsive to FSH. Theca cells, under stimulation by LH, produce androgens, which subsequently diffuse into adjacent GCs. In GCs, FSH promotes the expression of the enzyme CYP19A1 (aromatase), which catalyzes the conversion of androgens to estrogens [7]. Increased expression of CYP19A1 within GCs is recognized as a characteristic marker of a normal pre-ovulatory follicle [8]. After ovulation, LH promotes differentiation of Graafian follicle into corpus luteum which produces progesterone hormone. Increased levels of estrogen at mid-cycle give positive feedback to anterior pituitary to produce more LH. Finally increased level of estrogen and progesterone hormone gives negative feedback to anterior pituitary and to stop FSH, LH production and hypothalamus to stop GnRH production. But this hormonal control may get disrupted by poor lifestyle, diet or sometimes by environmental factors that gives rise to most common metabolic, endocrine disorder in female before menopause termed as polycystic ovarian syndrome (PCOS) [17].

Polycystic ovarian syndrome (PCOS) is the current epidemic that impacts an estimated 6-13% women during their reproductive years and up to 70% affected women remain undiagnosed worldwide [18]. PCOS is a polygenic, polyfactorial, systemic, inflammatory, dysregulated steroid state and autoimmune disease. Even though the etiology of this endocrinopathy is not clearly understood [15] or can't be cured, but symptoms still can be improved by lifestyle changes, medication or fertility treatments. The most prominent manifestations of PCOS include hyperandrogenism and insulin resistance (IR) [19]. Women with PCOS often suffer with a cluster of symptoms such as irregular or absent menstrual cycle, ovulatory dysfunction/chronic anovulation [20], hirsutism, obesity, type 2 diabetes, gestational diabetes, metabolic syndrome, hypertension [4], multiple fluid filled cysts, androgenic alopecia [17]. The most defining feature of PCOS is low level of CYP19A1 (aromatase) [9] and IR [20].

Researches have shown that in PCOS condition, the concentration of estradiol and CYP19A1 is prominently lower than that of normal follicles [9]. Apart from these, insulin

resistance (IR) is a major symptom of PCOS. IR refers to a state where the body cells do not respond optimally to normal insulin levels. It results in hyperinsulinemia or excessive insulin in blood stream, and can lead to diabetes mellitus. IR and hyperinsulinemia, along with inflammatory conditions in PCOS can promote abnormal androgen production, disrupted normal folliculogenesis and irregular menstruation, thus playing significant role in PCOS pathogenesis. The hyperandrogenism seen under PCOS condition can be attributed to high levels of androgens due to low levels of aromatase and also high levels of AR (androgen receptor), as has been previously observed under both *in vivo* and *in vitro* condition [8]. Along with it, elevated level of insulin upon IR may increase the level of free insulin-like growth factor (IGF-1) and together they interact with a receptor, IGF-1R. This inhibits AR repressor (FOXO1) causing an augmented AR transcriptional activity [6], thus aggravating the symptoms associated with hyperandrogenism.

GCs, often overshadowed by their oocyte counterpart, are inevitable architects of ovarian physiology, coordinating an intricate network of hormonal signalling, cellular differentiation, and follicular maturation that forms the foundation of female fertility [10]. Development of functional GCs can be traced back to the incidence of folliculogenesis that begins in a 4 months old female foetus where primordial follicles start to accumulate in the foetal ovary and generate the resting follicle pool (RF) [21]. Primordial follicles have simple structure containing oocyte arrested at prophase 1 and a single layer of squamous GCs around it, confined under basement membrane [22]. In subsequent stages of folliculogenesis, the GCs become cuboidal and gets differentiated into – mural GCs, located around the oocyte; and cumulus GCs, facing the antrum follicle [23]. Cumulus granulosa cells (CCs) further differentiate into corona radiata cells, which can support and guide sperm into the egg during fertilization [10]. In spite of the facts the both MGCs and CCs have arisen from the same progenitor precursor cells, MGCs and CCs have significant functional differences [24]. During the early stages of oocyte development, the MGCs synthesize estrogen (estradiol) for the development of female secondary sexual characteristics and regulation of reproductive cycle [20]. CCs are primarily responsible for providing environmental support for oocyte maturation. They establish gap junctions which allow oocytes through and permit the two-way conduction of information between GCs, enable metabolism and nutrient exchange [10]. Together the GCs give metabolic support to the developing oocyte by acquiring glucose from the surrounding tissues via the GLUTs, present on their cellular membrane, resulting in pyruvate and lactate production via glycolysis. This is the primary source of energy for proper folliculogenesis [11].

Since glucose is a key fuel and an important metabolic substrate that regulates gene transcription, enzyme activity, hormone secretion and gluco-regulatory neuron activity in mammals [11], any change in its regulation may have altered metabolic implication. It is important to note that differential glycolysis is one of the major consequences of PCOS. Differential expression of glycolytic enzymes in endometrial tissues affected by PCOS has been observed [15] but evidences supporting the same in case of local ovarian level or GCs surrounding the oocyte are yet to be researched.

For glycolysis in the GCs to occur properly and support folliculogenesis under normal physiologic condition, two most important glycolytic enzymes that are crucial, are glyceraldehyde-3-phosphate dehydrogenase (GAPDH) and phosphoglycerate kinase 1 (PGK1) [12]. In glycolysis, GAPDH catalyzes the conversion of glyceraldehyde-3-phosphate (GAP) into 1,3-bisphosphoglycerate (1,3-bis PG). GAPDH catalyzes the first redox reaction in glycolysis by producing NADH by reducing NAD^+ and oxidizing GAP [12]. On the other hand, PGK1 catalyzes the first ATP producing reaction in glycolysis by conversion of 1,3-bis PG into 3-phosphoglycerate and prevents the pathway from going backward, thus optimally regulates the glucose metabolism in GCs and supplies energy for folliculogenesis [11]. Further, PGK1 also has vital interactions with AR [13]. During folliculogenesis, AR is very important for follicular growth which is mostly expressed on the surface of ovarian GCs [15]. PGK1 is known to regulate glucose metabolism in coordination with AR [14]. In another study, an elevated abundance of PGK1 has been observed in luteinized GCs from PCOS patients as well as in ovarian tissues of PCOS-like mouse models, regulated glucose metabolism in them and further degrades the PCOS-like symptoms in mouse. It has been hypothesized that there might be a positive correlation between PGK1 and AR [13]. However, the precise mechanisms through which PGK1 governs glucose metabolism in GCs, contributing to IR and other metabolic complications associated with PCOS, remain largely elusive [14].

As mentioned earlier, besides serving as a vital energy force, glucose is also a critical metabolic substrate that influences gene expression, modulates enzymatic functions, governs hormone release and impacts the activity of gluco-regulatory neurones in mammals [25]. In mammalian cells, the movement of glucose across the plasma membrane is mediated by a specialized family of proteins known as glucose transporters (GLUTs), which facilitate its efficient transport [11]. Previous studies showed that expression of GLUTs changes in PCOS condition. Under normal physiology, GLUT-1 is predominantly present on the surface of GCs. But in PCOS condition, GLUT-4 is upregulated and GLUT-1 is

downregulated [11]. As a result it can be hypothesized that glucose uptake will also be increased. Nonetheless, the expression profiles and functional roles of the more recently identified GLUT isoforms remain comparatively underexplored within ovarian tissues. Researchers have shown that in mouse, the transition of primordial to primary follicles is accompanied by increased energy requirement or glycolysis in GCs along with upregulation of GLUT-4 (glucose transporter-4) and glycolysis rate-limiting enzymes such as hexokinase 1 (HK1), phosphofructokinase (PFKL) and pyruvate kinase M2 (PKM2). The mTOR signaling is crucial here to provide enough energy for increased metabolism and stimulate folliculogenesis [26]. Also, in PCOS patients, GLUT-4 protein expression is found to be decreased in adipocytes while GLUT-1 expression is increased in skeletal muscles. Reduced expression of GLUT-4 is also found due to reduced level of estrogen in uterus [11].

Previous studies by Saha et al and group (2021) have shown that upregulated levels of AR and downregulated levels of CYP19A1 (aromatase) are reverted upon treating GCs or PCO rats with a herbal drug named as thymoquinone (TQ) [8]. Taken together, these considerations form the basis for the present study, which seeks to investigate alterations in glycolytic enzymes and GLUT expression at the local ovarian level under polycystic ovarian condition utilizing an established PCOS model [8] based on the murine granulosa cell line KK-1. This study can potentially offer deeper insights into cellular metabolic disruptions that contribute to the onset of PCOS, and the potential therapeutic effect of TQ on the same if any.

3. AIMS & OBJECTIVES

As evident from the existing literature, women with PCOS exhibit lower CYP19A1 (aromatase) expression, elevated androgens and AR ensuing activated androgen-AR signaling implicated in impaired folliculogenesis that causes chronic anovulation and a chronic accumulation of androgens within the female body leading to hyperandrogenism [8]. The normal development of follicles and the consequential maturation of oocyte depends mainly on the uptake of glucose from the surrounding tissues by GCs via GLUTs on their cell membrane. Interestingly, AR-androgen axis under homeostasis has been implicated to regulate glycolysis.

Thus, we hypothesize that: "Elevated AR expression under polycystic ovarian condition dysregulates glycolysis resulting in impaired folliculogenesis".

The objective of the present study is as follows:

"To elucidate the effect of elevated AR expression on glycolytic factors and downstream targets with special emphasis on key glycolytic enzyme PGK1 under PCO condition".

4. MATERIALS AND METHODS

4.1 Materials

4.1.1 Chemicals and Kits used:

- Regular lab reagents were either purchased from HiMedia Laboratory Pvt Ltd. (Maharashtra, India) or Sisco Research Laboratories Pvt Ltd. (Maharashtra, India).
- PureZol, Biorad was used for RNA extraction.
- iSCRIPT^{TM} RT-PCR Kit with SYBR Green from BIO-RAD was used for cDNA preparation and PCR amplification.
- Secondary antibodies were obtained from Sigma Aldrich Chemicals Pvt. Ltd. (USA) and Cell Signaling Tech. (USA), AbClonal.
- Water used for preparing buffers, reagents was either autoclaved triple distilled or Milli Q (obtained from water purification system, Millipore, MA, USA).
- Cell culture plastic wares were obtained from Corning-Costar Inc. (Sigma/Merck USA).
- PVDF membranes for filtering media and 0.22 µM membrane filters were obtained from Merck Millipore (MA, USA).
- Filtration unit and isopropanol cryobox were purchased from Tarsons (India).
- 2-NBDG dye [2-(N-(7-Nitrobenz-2-oxa-1,3-diazol-4-yl)Amino)-2 deoxyglucose] was purchased from MedChemExpress (MCE), Cat. No.: HY-116215
- DHT (Dihydrotestosterone) was purchased from Supelco.
- Enzalutamide was purchased from MedChemExpress (MCE), Cat. No.: HY-70002

4.1.2 Equipment used:

- Colibri nanodrop instrument was used for estimating RNA concentration and purity.
- First strand synthesis (cDNA preparation) was performed in Biorad S1000 Thermal Cycler.

- qRT-PCR was performed using CFX connect Real-Time Detection System.
- Fluorescence microscope Leica DM6 B by Leica Microsystems CMS GmBH, Germany.
- BIORAD Chemidoc^{TM} MP Imaging System.

4.2 Methods

4.2.1 Mammalian cell culture:

(A) Maintenance of murine granulosa cell line, KK-1:

The KK-1 granulosa cell line was developed in the laboratory of Dr. Ilpo Huhtaniemi, University of Turku, Finland and was procured from Dr. Nafis Rahman. Cells were maintained in high glucose DMEM (Dulbecco's Modified Eagle's Medium), containing 4.5 gm/L glucose. The media was supplemented with 10% FBS (Origin South America, PAN-Biotech, Germany), 50 IU/mL penicillin, 50 µg/mL streptomycin and 0.25 µg/mL amphotericin B in tissue culture plates. The cultures were grown at 37°C in a humidified atmosphere with 5% CO_2 and 95% air. The cells were routinely passaged to maintain a monolayer culture by detaching from the plastic surfaces of cell culture plates by trypsinization. Cells were also sub-cultured regularly.

(B) Creation of hormone primed *in vitro* models using KK-1 cell line (UT, SO, PCO, TQ):

The hormone treated *in vitro* models of super-ovulated (SO), polycystic ovary (PCO)/anovulatory condition and thymoquinone (TQ) treated PCO models were created as per established protocol [8]. First the cells were seeded on 100 mm cell culture plates and those plates undergone media change after 6 hours of seeding (0 hour). After 40 hour of cell growth, cells were treated with hCG (10 IU/mL) i.e. hormone primed in order to mimic the physiological condition and these are termed as SO. For generating the PCO experimental set, the KK-1 cells were treated with both hCG and an anti-progestogen drug mifepristone, also known as RU486 (10 µM or 50 µM), at 40 hour of growth. For the thymoquinone (TQ) treated PCO model, the cell were treated with TQ (10 µM) beforehand, at 36h of growth. Next it was treated with hCG and RU486 at 40 h of growth. All those cells were harvested after 8 hours of i.e. 48 hours of growth. Untreated (UT) KK-1 cells were grown for 48 hours for using as a control (**Figure 4.2A**).

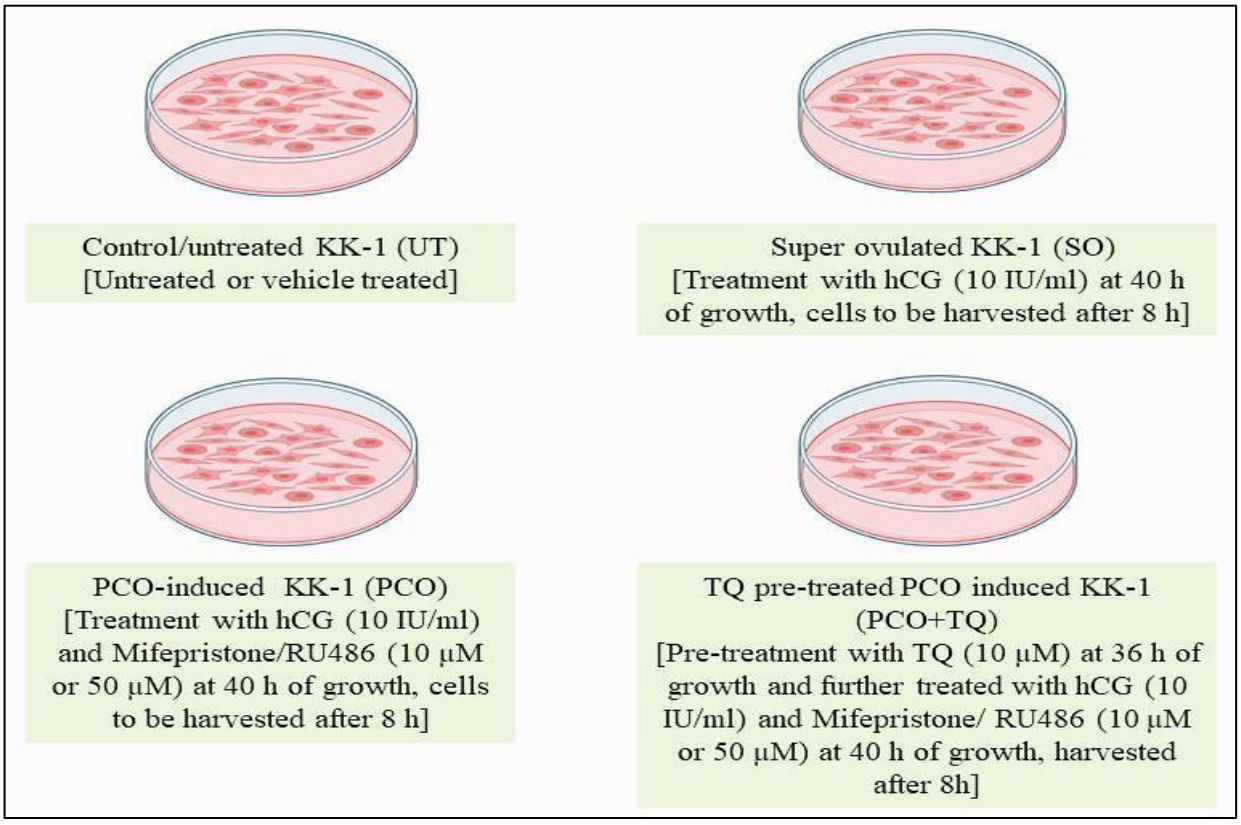
Control/untreated KK-1 (UT)
[Untreated or vehicle treated]
Super ovulated KK-1 (SO)
[Treatment with hCG (10 IU/ml) at 40 h of growth, cells to be harvested after 8 h]
PCO-induced KK-1 (PCO)
[Treatment with hCG (10 IU/ml) and Mifepristone/RU486 (10 µM or 50 µM) at 40 h of growth, cells to be harvested after 8 h]
TQ pre-treated PCO induced KK-1 (PCO+TQ)
[Pre-treatment with TQ (10 µM) at 36 h of growth and further treated with hCG (10 IU/ml) and Mifepristone/ RU486 (10 µM or 50 µM) at 40 h of growth, harvested after 8h]

Figure 4.2A: Generation of different experimental sets (Control, Super-ovulated, PCO induced and TQ pre-treated) utilizing KK-1 cell line

(C) Treatment of cells with dihydrotestosterone (DHT):

Dihydrotestosterone (DHT) is a potent androgen that binds to the androgen receptor (AR) and activates it. Once activated, AR translocates to the nucleus and acts as a transcription factor to regulate various gene expressions governed by AR itself. Enzalutamide is a non-steroidal, anti-androgen that competes with DHT to bind to AR. Upon binding, it prevents AR activation, inhibits its nuclear translocation and blocks AR-mediated transcription of androgen-responsive genes. In order to examine any change in expression of PGK1 upon AR activation, KK-1 cells were treated with DHT, a known agonist of AR signaling. Cells were seeded on four 100 mm cell culture plates and they were treated as follows – VT (vehicle treated), KK-1+DHT (dihydrotestosterone), KK-1+AR Blocker (enzalutamide) and KK-1+DHT+enzalutamide. The concentration of DHT and enzalumamide used for treatment are 50nM and 5µM respectively. The treatment was given for a period of 24h and subsequently the cells from all four experimental sets were harvested for protein sample preparation.

4.2.2 RNA extraction, estimation & purity checking:

All the four cell samples (UT, SO, PCO, TQ) were treated with TRIzol reagent and taken into fresh 4 microcentrifuge tubes and were centrifuged for 2 minutes at 13000 rpm at 4°C. After centrifugation, the supernatant was collected and put into fresh four microcentrifuge tubes and labeled accordingly. Next 0.2 ml (200 µl) chloroform ($CHCl_3$) was added to each tube and contents were mixed thoroughly by rigorously shaking and inverting the tubes for 30 seconds (tubes should be vortex to avoid RNA degradation into pieces) and incubated at room temperature (RT) for 5 minutes and mixing periodically. Centrifuge each tube at 12000 g for 15 minutes for phase separation. The aqueous phases from each tube were carefully transferred to fresh microcentrifuge tubes without disturbing the interphase. Next 0.5 ml (500 µl) isopropanol was added to each tube followed by thorough mixing and incubate at RT for 5min. The tubes were centrifuged at 12000 g for 10 min at 4°C. After centrifugation, supernatant was discarded and pellet was resuspended with 1 ml of 75% ethanol. Samples were vortexed and centrifuged 7500 g for 5 minutes at 4°C and the supernatant was discarded, pellet was allowed to air dry completely by inverting the tubes keeping lids open on a clean, dry piece of tissue paper. After drying the pellet, it was resuspended in nuclease free water (NFW), properly mixed by pipetting. This newly extracted RNA samples were kept at RT and stored in ice before estimation. The absorbances of the samples were measured at 260 nm and concentration (ng/µl) using Colibri Nanodrop instrument. Along with that, the purity of prepared samples was checked by measuring the absorbance ratios $A_{260/280}$ and $A_{260/230}$. cDNA was also prepared according to the calculations in the below table. Remaining RNA samples were stored at -80°C.

RNA Quantification				
Sample	**OD 260/280**	**OD 260**	**Concentration (ng/µl)**	**Volume required for 5 µg (5000/conc.)**
UT	1.92	16.47	658.91	7.58
SO	1.98	12.31	492.57	10.15
PCO	1.98	8.78	351.10	14.24
TQ	1.89	27.40	1096.06	4.56

Table 1: Table showing Nanodrop readings for RNA concentration, $A_{260/280}$ reading and volume (µl) required for 1 µg of RNA from ovary samples to be used for cDNA preparation.

Sample	RNA	NFW	Mastermix (reverse transcriptase+buffer)
UT	7.58	7.42	5
SO	10.15	4.85	5
PCO	14.24	0.76	5
TQ	4.56	10.44	5

Table 2: Table showing the exact volume of reagents for cDNA preparation reaction.

4.2.3 Preparation of cDNA and gene amplification by qPCR:

After quantification of RNA samples, cDNA was prepared using BIO-RAD S1000 thermal cycler and also iSCRIPT^{TM} RT-PCR Kit with SYBR Green from BIO-RAD. The complete reaction mixture was incubated in the thermal cycler using the following protocol as shown below –

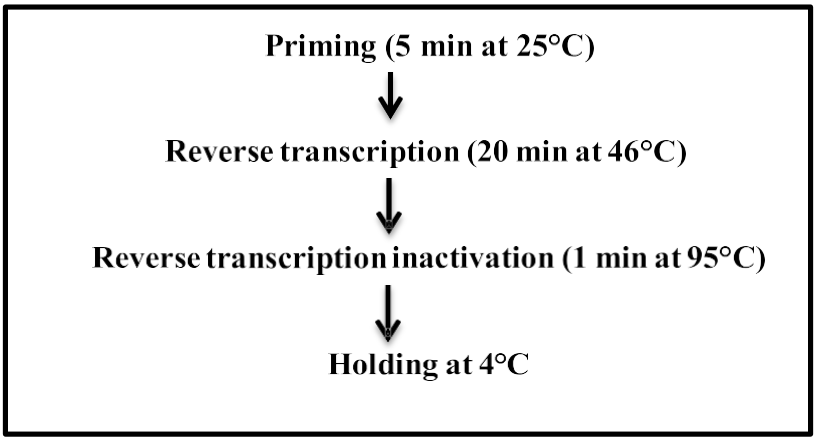

Figure 4.2B: Flowchart of cDNA preparation protocol

- List of primers used for qPCR

Gene Name	Direction	Primer sequence
PGK1 (mouse)	Forward	5'-GATCAAGGCTGCTGTTCCAA-3'
	Reverse	5' GAACAGAACATCCTTGCCCA-3'
GAPDH (mouse)	Forward	5'- TGTGTCCGTCGTGCATCTGA-3'
	Reverse	5'- CCTGCTTCACCACCTTCTTGA-3
GLUT-4 (mouse)	Forward	5'-CGGGCTCTGACGATGGGGA-3'
	Reverse	5'-TCAATCACCTTCTGTGGGGC-3'
Actb (mouse)	Forward	5'-ATGACCCAGATCATGTTTGAG-3'
	Reverse	5'-AGGATGGCGTGAGGGAGAG-3'

Table 3. Table showing the primer sequences of genes for amplification

The cDNA samples were first prepared by diluting at a ratio of 1:10 in two different 200 µl microcentrifuge tubes. Next the samples were diluted further by adding NFW of appropriate amount, mixed by pipetting to ensure homogeneity. Subsequently, two fresh centrifugation tubes were taken and labeled with the corresponding target gene names and the qPCR mastermix was aliquoted in each tube. Also, equal volumes of forward and reverse primers were added in their respective tubes. All the components were mixed very well by pipetting. A sterile 96-well qPCR plate were then used and labeled appropriately with the target genes and samples in triplicate manner where the total reaction volume of each well was 10 µl. The mastermix plus primers mixture was horizontally dispensed in each well in the volume of 6 µl and the sample plus NFW mixture was dispensed vertically in each well in the volume of 4 µl. The plate was then sealed securely and placed into CFX connect Real-Time Detection System. Protocol was set as follows – Initial denaturation at 95°C for 30 sec, cycle denaturation at 95°C for 5 sec, cycle annealing at 60°C and extension at 72°C for 30 sec and this was repeated for 40 cycles. The graph was also analyzed.

4.2.4 Protein sample preparation from experimental set cell lysates and concentration estimation:

The experimental sets of cells were grown in 100 mm plates, and treatment was given as per the lab protocol. For each set, 3 confluent 100 mm cell culture plates were taken and the existing exhausted media was discarded from the plates. Then each plate was washed with 1X PBS. To the plates, 1 ml trypsin was added and incubated at 37°C, 5% CO_2 for 2-3 minutes. After 2-3 minutes of incubation, 1 ml fresh DMEM containing 10% FBS was added to the plates to make a uniform cell suspension. The cell suspension were taken in 15 ml falcons and centrifuged at 700 rpm for 5 minutes and the supernatant was discarded. Then 200 µl 1X PBS was added to the cell pellet obtained and it was resuspended by pipetting to wash out the residual DMEM media. The suspension was then collected in microcentrifuge tubes and centrifuged at 800 rpm for 5 minutes. The supernatant was discarded and the pellet was stored at -20°C.

The cell pellets were treated with RIPA buffer and kept in icebox. Next, they were slowly rocked until the mixture turns transparent. The cells were centrifuged at 13000 rpm for 15 minutes at 4°C. Fresh microcentrifuge tubes were prepared and labeled in which the supernatant was collected. Similarly, protein was extracted from DHT treated samples.

Then protein estimation assay was performed using Bradford reagent. Protein content of each sample was estimated using standard Bradford method with known standard curve of bovine serum albumin (BSA). The concentration of the samples was determined from the equation received from the standard curve.

Following protein quantification, one-fourth the volume of 5X SDS sample buffer was added to each microcentrifuge tube containing the respective samples. The mixtures were then incubated in a dry bath at 95°C for 15 minutes to ensure protein denaturation, promptly chilled on ice to stabilize the denatured proteins, and centrifuged at 13,000 rpm for 15 minutes at 4°C. The resulting supernatants were carefully collected and preserved at −20°C for further analysis.

Samples	Average OD at 595 nm
Blank	0
BSA 2	0.208667
BSA 5	0.369667
BSA 10	0.427333667
BSA 15	0.610333667
BSA 20	0.673000333
UT	0.67
SO	0.67
PCO	0.70
TQ	0.69

Table 4: Table showing average OD at 595 nm after subtracting the Blank reading by Bradford Assay

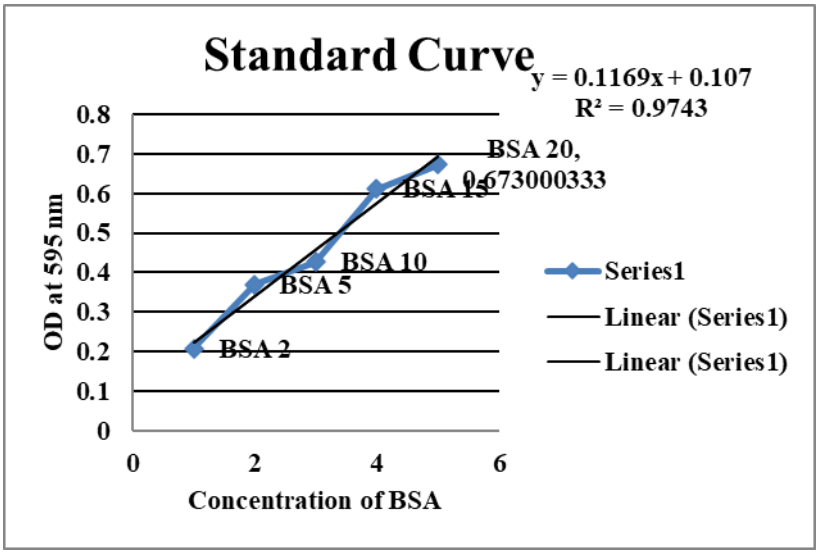

Figure 4.2C: BSA standard Graph obtained from BSA known Concentration

4.2.5 Sodium dodecyl sulfate polyacrylamide gel electrophoresis:

Linear slab gel electrophoresis under denaturing condition was performed to separate the protein bands. Suitable volume of samples was loaded into the respective wells of the gel from each of the samples – UT, SO, PCO, TQ. Along with that, appropriate amount of protein ladder was also loaded. The proteins were stacked at pH 6.8 in 4% stacking gel containing 4% acrylamide, 0.106% N, N'-methylene bis-acrylamide, 0.125 M Tris-HCl, 0.01% TEMED and 0.1% ammonium per sulphate (APS). The resolving gel was 12.5% and had pH of 8.8, consisting of 12.5% acrylamide, 0.33% N, N'-methylene bis-acrylamide, 0.375 M tris-HCl, 0.01% TEMED and 0.1% APS. Proteins were electrophoresed in running buffer of pH 8.3, containing 0.025 M Tris-base, 0.192 M glycine and 0.1% SDS. The voltage was kept at 60 V when the bands were in stacking gel and increased to 120 V when bands reached the resolving gel. This voltage was maintained throughout the run.

4.2.6 Western blotting:

After electrophoretically separating the proteins, the bands were transferred onto a PVDF membrane, which was first blocked for 1 hour with 3% BSA solution dissolved in PBS. Then the blot was washed with PBST (0.05% tween 20 dissolved in PBS) for 5 minutes on fast rocker. Next the blot was incubated with primary antibody (anti-rabbit-GLUT-1, anti-rabbit-GLUT-4, anti-rabbit-PGK1, anti-rabbit-β actin) dissolved in 1.5% BSA solution overnight at 4°C on slow rocker. Then the blots were washed with PBST thrice, each for 15min on fast rocker. Next the blot was incubated with secondary antibody (HRP or AP conjugated secondary antibodies were used that were either raised in mice or rabbit, as per requirement) dissolved in 1.5% BSA solution at room temperature for 1 hour on slow rocker followed by 3 PBST washes, each for 15 minutes. Next the blots were developed by using appropriate substrates and their respective protocols.

4.2.7 Detection of protein by enhanced chemiluminescence (ECL) or colorimetry:

For detecting the blots with immune complexes containing HRP tagged secondary antibodies, enhanced chemiluminescence was used. The blots were treated with ECL reagents – 22 µl p-coumaric acid (90mM), 50 µl luminol (250 mM) and 3 µl (30%) H_2O_2

dissolved in 10ml Tris- buffer (pH 8.5). For detection of protein bands, an instrument called BIORAD ChemiDoc^{TM} MP Imaging System was used and chemiluminescence was captured.

For detecting the blots with immune complexes containing alkaline phosphatase (AP) tagged secondary antibodies, colorimetric detection protocol was used. AP reaction mix was prepared by dissolving 66 µl NBT (50 mg/ml) and 33 µl BCIP (50 mg/ml) into 10 ml AP buffer (pH 9.5). Next the AP reaction mix was added to the boxes containing the blots and covered fully with aluminum foil as these are light sensitive and optimal reaction needs dark environment. Blots were incubated on slow rocker until bands are visible.

4.2.8 Immunofluorescence studies:

The cells were seeded onto the surface of coverslips, kept in a 12 well. Then the media was gently aspirated out of the wells and the wells were washed with 1X PBS. The cells were fixed with chilled methanol and stored at -80°C. Next day, the fixed cells were observed under microscope and the coverslips were transformed to another fresh 12 well plate where in each well 1 ml paraformaldehyde (PFA) was added. Incubate at 37°C for 15 minutes. Next PFA was removed by adding 1X PBS to the wells and washed by shaking with palms until the smell of PFA is faded. Next, 1 ml Glycine was added into each well and incubated at 37°C for 5 minutes followed by washing with PBS. Next, 1 ml Triton X100 was added to create pores in the cell membrane so that cells become receptive to antibodies. It was incubated at 37°C for 1 min followed by removal of the Triton X 100 with PBS wash. After that, 12 parafilm squares were cut in the size of the wells and those squares were placed on the lid. On each square, 50 µl blocking solution (3% BSA+PBS) was placed and the coverslips were placed with the help of needle and forceps such that the cell side faces the blocking solution. The lid was incubated in a moist chamber for 1 hour at 37°C followed by washing with PBS. Next on each strip, 50 µl primary antibody (anti-mouse-AR and anti-rabbit-PGK1 in one set and in another set anti-rabbit-GLUT-4) solutions were added and coverslips were put back in previous manner. It was incubated overnight at 4°C. Next day, coverslips were washed with 1X PBS thrice each for 10 minutes. The coverslips were incubated with 50 µl fluorescent tagged secondary antibody solution (anti-rabbit-green, anti-mouse-red in case of co-localization studies between AR and PGK1, and anti-rabbit-red in case of GLUT-4) in a moist chamber at 37°C for an hour followed by washing with 1X PBS twice for 20 minutes. Meanwhile, the nuclei were

stained with DAPI solution. Next, on a clean slide approximately 20 µl of 50% glycerol was added and coverslips were carefully placed on slide with cell facing the glycerol. Coverslips were sealed with clear nail polish and examined under microscope.

4.2.9 Glucose uptake assay using 2-NBDG:

Glucose uptake in live cells was assessed using the fluorescent glucose analog 2-NBDG [2-(N-(7-Nitrobenz-2-oxa-1,3-diazol-4-yl)Amino)-2-deoxyglucose]; following previously established protocols [27] with minor modifications. Cells were seeded onto coverslips in 12 well plates (Corning) and cultured to ~60% confluence under standard conditions (37°C, 5% CO_2). The cells were pre-treated with TQ (10 µM) at 36 h of growth. After 40 h of growth, cells were treated with hCG (10 IU/ml) and RU486 (10 µM or 50 µM), to create SO and PCO models, as per the established protocol [8] described earlier. At 48 h of growth, media was discarded and cells were washed with PBS. Cells were incubated with PBS at 37°C for 10 minutes. Next on clean slides, 50 µl of 2-NBDG (100 µM) was dispensed and cover slips were placed with cell sides facing the 2-NBDG. Cells were incubated for 15 minutes in dark. After incubation, coverslips were washed with PBS to remove unincorporated dye. The washed coverslips were put back on the respective slides and sealed with clear nail polish. Next, they were immediately subjected to live-cell fluorescence imaging (excitation: 467 nm, emission: 538 nm).

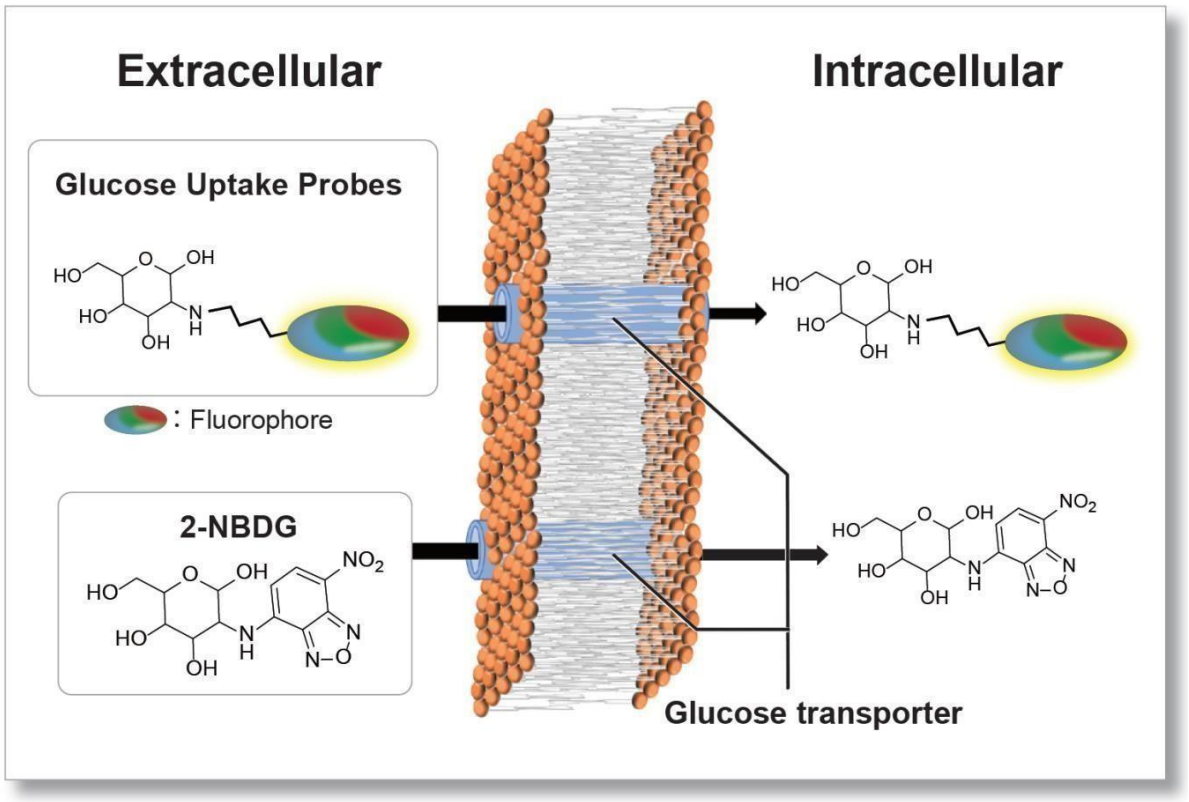

Figure 4.2D: Image showing the working principle of 2-NBDG
(Image source: https://www.dojindo.com/JP-EN/products/UP02/img/up02_principal.png)

4.2.10 Statistical analysis:

ImageJ software was used to analyze band intensities of the immunoblots and after normalization with the loading controls, relative fold changes were calculated accordingly. All data are represented as mean ± SD of observations from different experiments in triplicates (n=3). Unpaired students t- test was performed using GraphPad, Quickcalcs software. Difference at a level of $^{*}p < 0.05$, $^{**}p < 0.01$ (or as indicated in the Figures) between groups are considered statistically significant.

5. RESULTS AND DISCUSSION

5.1 Differential expression of the glycolytic enzymes GAPDH and PGK1 under PCO condition:

Androgen-AR axis has been implicated to play a crucial role in tissue-specific regulation of glucose metabolism [28] which includes cardiomyocytes [29], skeletal muscles, hepatocytes, adipose tissues as well as metabolic centers present in hypothalamus [30]. A

gender specific differential regulation of glucose homeostasis mediated by androgen-AR axis has also been perceived. Androgen deficit in males reportedly leads to altered metabolism and type2 diabetes (T2D), while excess androgen systemically triggers T2D in females [30]. Previous work in the lab has elucidated an upregulated expression of AR in the GCs under both *in vitro* and *in vivo* PCO conditions ([8] and Unpublished Data). Thus, in order to understand the effect of elevated AR levels at the local ovarian levels, considering the crucial function of GCs in providing energy needs of the oocyte, expression of two key glycolytic enzymes GAPDH and PGK1 was analyzed both at the transcript and protein levels. The experiment revealed differential expression of GAPDH and PGK1 in the PCO experimental sets. GAPDH was significantly downregulated while PGK1 was significantly upregulated at both the transcript and protein levels in the PCO set in comparison to the super-ovulated (SO) controls. TQ treatment was able to revert back the condition considerably (**Figure 5.1**). This observation signifies impaired glycolysis under PCO condition. As the expression of GAPDH is downregulated, affecting energy harness during folliculogenesis; suggested upregulation in PGK1 may imply a compensatory mechanism against the same.

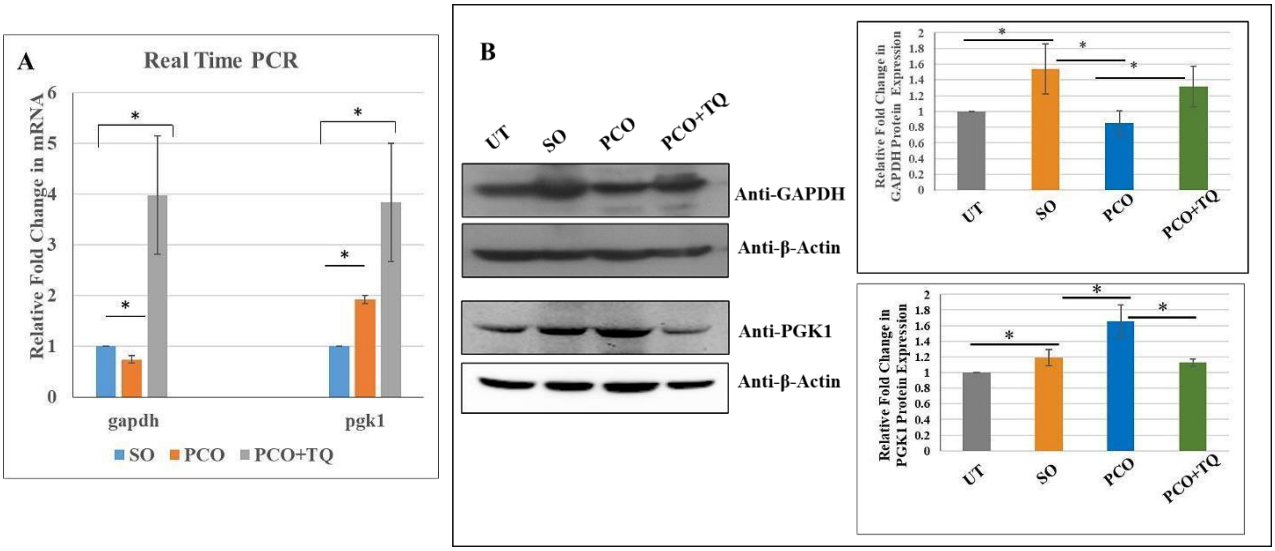

Figure 5.1: Differential expression of glycolytic enzymes GAPDH and PGK1 under PCO condition.
(A) Significant downregulation of GAPDH and upregulation of PGK1 was observed at the transcript level upon performing qRT-PCR. **(B)** Immunoblotting with whole cell lysates for both GAPDH and PGK1 along with loading control β-Actin confirmed the significantly downregulated expression of GAPDH under the PCO condition. While as observed at the transcript level, PGK1 expression was markedly upregulated in PCO set compared to SO at the protein level. TQ treatment was able to restore the levels of both the enzymes similar to that of the SO experimental sets. Band intensities of the respective samples were analyzed though ImageJ and normalized with β-Actin intensities and Students T-test was performed for statistical analysis.

5.2 *In silico* analysis predicting potential interaction between AR and PGK1:

Recent reports suggest glycolytic enzyme, PGK1 stabilizes AR by interacting with it [17]. Elevated AR levels under PCO condition combined with the present observation of increased expression of PGK1 in the GCs under PCO instigated us to examine the binding potential of PGK1 and AR via *in silico* approaches. PDB files of both the protein and the ligand was downloaded and molecular docking by H-dock software was performed. The best interactive model revealed a docking score of -224.79 between AR and PGK1 protein, which was further visualized by PyMOL. The score indicates a strong potential interaction between the two (**Figure 5.2A**).

It has been predicted that PGK1 mediated stabilization of AR, a nuclear receptor; can take part in the positive feedback loop leading to augmented transcription of PGK1 [11]. Thus, using bioinformatic tools, we further embarked upon analysis of any probable binding of AR with the PGK1 promoter. PGK1 promoter sequence was downloaded from EPD database. Utilizing the bioinformatics tool, JASPAR, AR binding site at the PGK1 promoter sequence and its relative binding score was predicted. The analysis revealed relative score of 0.8 between AR and PGK1 promoter sequence predicting possible AR binding to PGK1 promoter; which might signify AR's role in elevating PGK1 expression under PCO condition (**Figure 5.2B**).

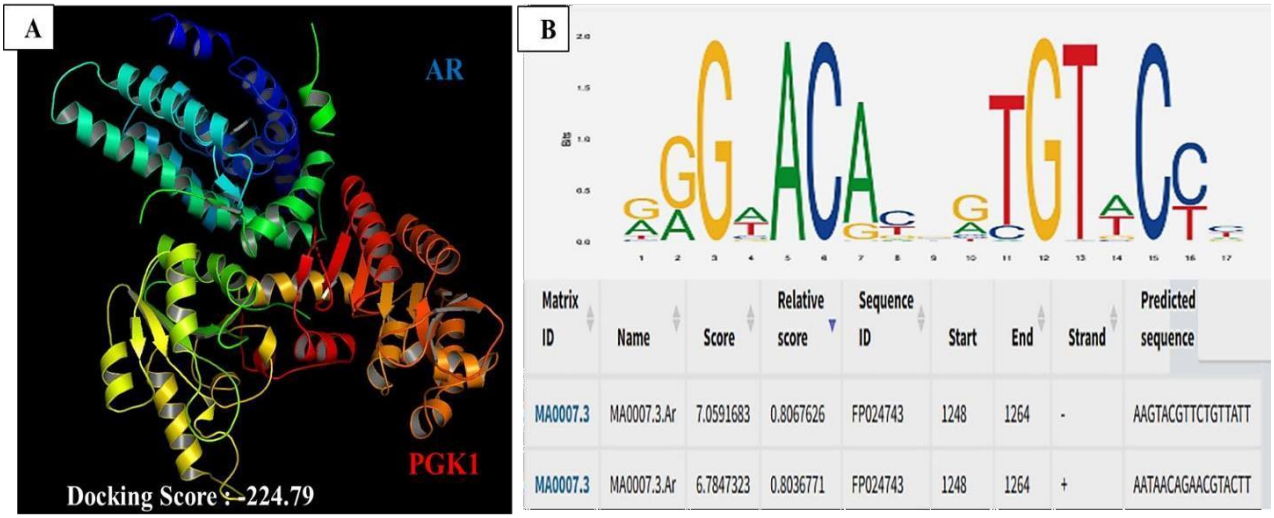

Matrix ID	Name	Score	Relative score	Sequence ID	Start	End	Strand	Predicted sequence
MA0007.3	MA0007.3.Ar	7.0591683	0.8067626	FP024743	1248	1264	-	AAGTACGTTCTGTTATT
MA0007.3	MA0007.3.Ar	6.7847323	0.8036771	FP024743	1248	1264	+	AATAACAGAACGTACTT

Figure 5.2: Predicted interaction between AR and PGK1 from bioinformatics analysis. **(A)** Molecular docking by H-dock software reveal a docking score of -224.79 between AR and PGK1 proteins, indicating strong potential interaction between the two. **(B)** Predicted sequence of AR and its relative binding score to PGK1 promoter sequence as predicted by JASPAR.

5.3 Augmentation of PGK1 expression upon DHT treatment and reversal upon treatment with AR-blocker enzalutamide in KK-1 cells:

The nuclear receptor, AR gets activated upon binding with its ligand (androgens), dimerizes and gets translocated to the nucleus. To decipher whether AR activation leads to increased expression of PGK1 in GCs, KK-1 cells were treated with the AR ligand dihydrotestosterone (DHT) in one set. In another set KK-1 cells were treated with both DHT as well as the AR blocker, enzalutamide, in order to prove that the augmented expression of PGK1, if any is due to activation of AR. Vehicle treated KK-1 and only enzalutamide treated KK-1 acted as controls for the experiment. The protein samples isolated from these treated sets were further subjected to SDS-PAGE followed by western blotting. Immunoblotting for PGK1 revealed a marked elevated expression of PGK1 upon activation of AR in the DHT treated cells, while DHT and enzalutamide treatment led to reduced expression of PGK1. This signifies that the upregulated expression of PGK1 is specifically due to AR activation, hence upon AR blocker, enzalutamide treatment there is a decline in PGK1 expression (**Figure 5.3**).

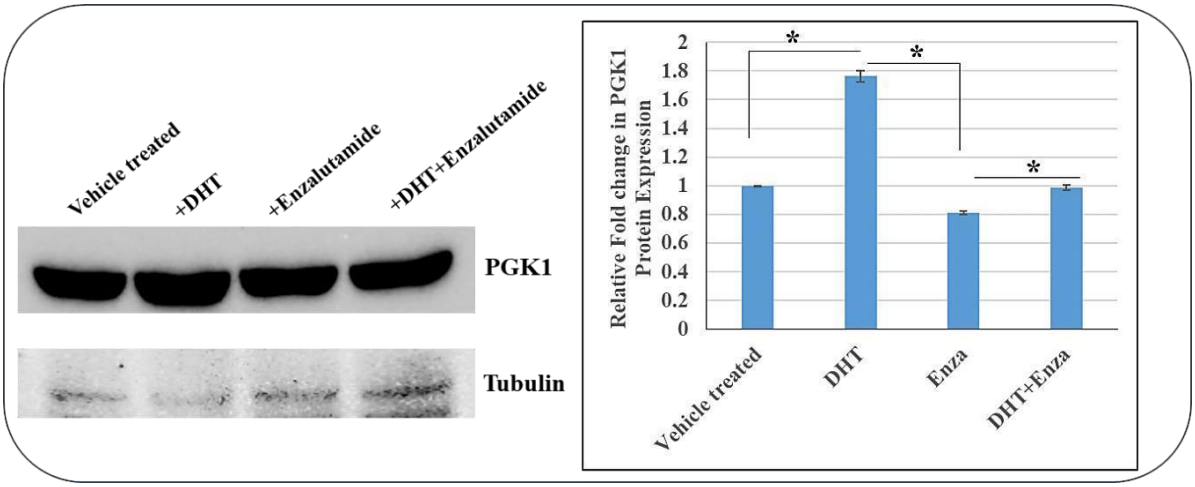

Figure 5.3: Modulation of PGK1 expression by DHT and AR blocker Enzalutamide. Expression levels of PGK1 significantly increased upon DHT treatment in KK-1 cells and are reversed upon co-treatment with Enzalutamide, indicating AR activation leads to PGK1 upregulation and confirming androgen-AR mediated regulation of PGK1 in GCs.

5.4 Elevated expression and nuclear localization of AR and PGK1 under PCO condition as evident from immuno-fluorescence analysis:

Taking cues from the *in-silico* analysis and the above experiment implying PGK1 expression is intensified upon AR activation, it was necessary to substantiate this observation, through investigation of the sub-cellular localization of AR and PGK1 in the experimental sets (SO, PCO and PCO+TQ). Immunofluorescence analysis revealed a distinctively elevated expression of both AR and PGK1, concomitant with our previous immunoblot data in the PCO set. Both the proteins were primarily localized in the nucleus under the PCO condition. Intensified co-localization of AR and PGK1 in the nucleus indicated by enhanced yellow colour was also observed in the KK-1 cells under the PCO condition (**Figure 5.4**); suggesting a positive correlation between these two factors.

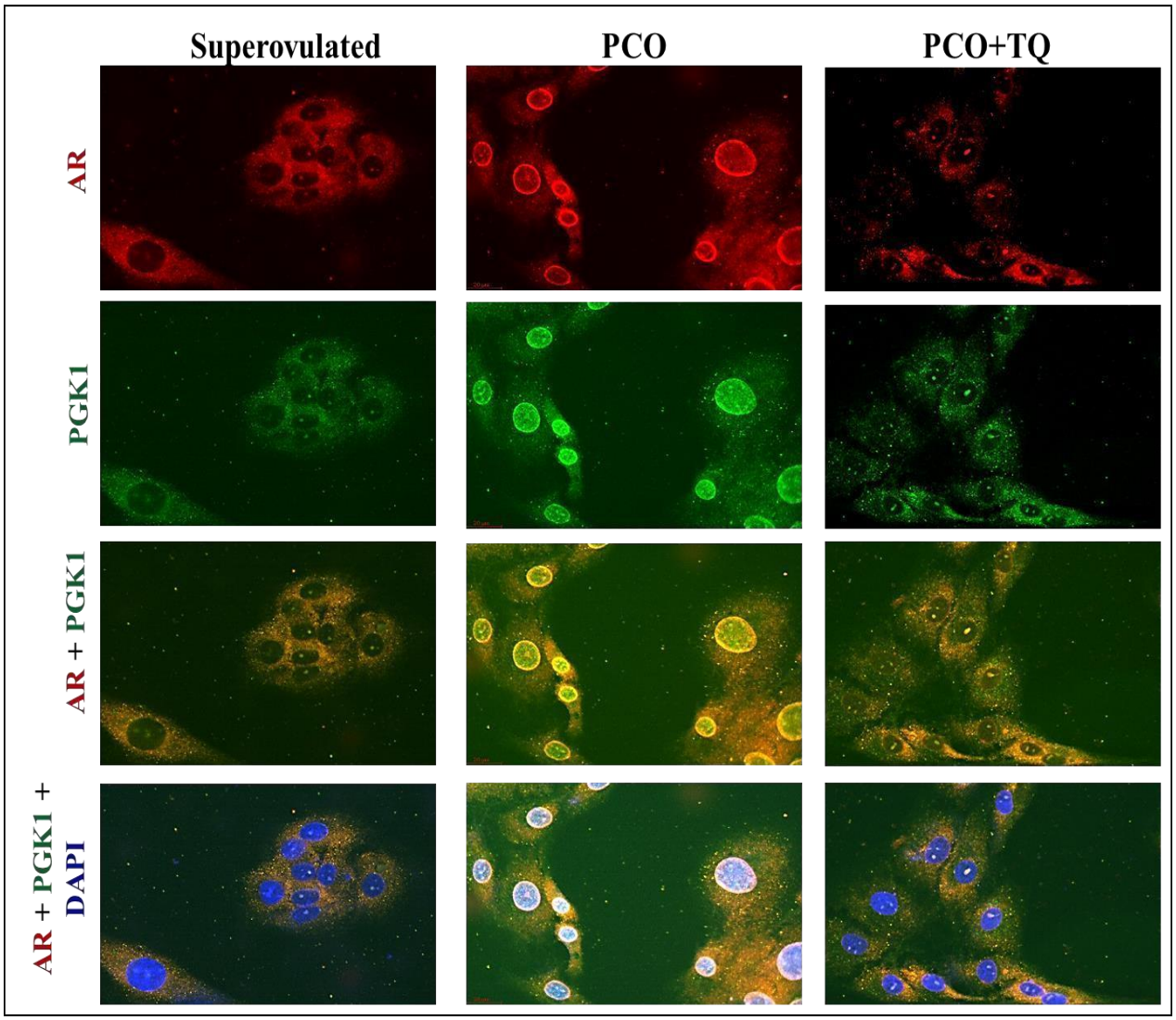

Figure 5.4: Immunofluorescence analysis shows nuclear co-localization of AR and PGK1 in PCO samples. Elevated expression of AR and PGK1 under PCO condition as evident from immuno-fluorescence analysis. Intense yellow staining in cells under PCO condition indicates co-localization of AR and PGK1. The observation implies probable AR and PGK1 binding and functional interaction.

5.5 Significant upregulation of glucose transporter GLUT-4 under PCO condition:

Reports suggest that among all the glucose transporters, GLUT-4 is differentially regulated during IR condition while GLUT-1 is constitutively expressed [13]. Thus, in order to check the expression status of GLUT-4 in the GCs under PCO condition, RNA was extracted from all the experimental sets and subsequently processed for cDNA preparation after purity check. Further, semi-quantitative PCR amplification was carried out using gene specific primers for the glucose transporter, GLUT-4 along with β-actin gene as the housekeeping control. The analysis revealed significant upregulation in GLUT-4 expression in PCO model compared to SO model, while significant yet minor reversal of this condition was observed in pre TQ treated set. The expression of GLUT-4 was significantly lower than that of the PCO sample upon TQ pre-treatment but significantly elevated than that of the SO sample (**Figure 5.5A**).

Cell lysates from the four experimental sets were further subjected to immunoblot analysis using antibody against GLUT-4, which also revealed a significantly elevated expression of GLUT-4 in PCO sample compared to SO. Markedly significant reversal was also observed upon TQ treatment (**Figure 5.5B**).

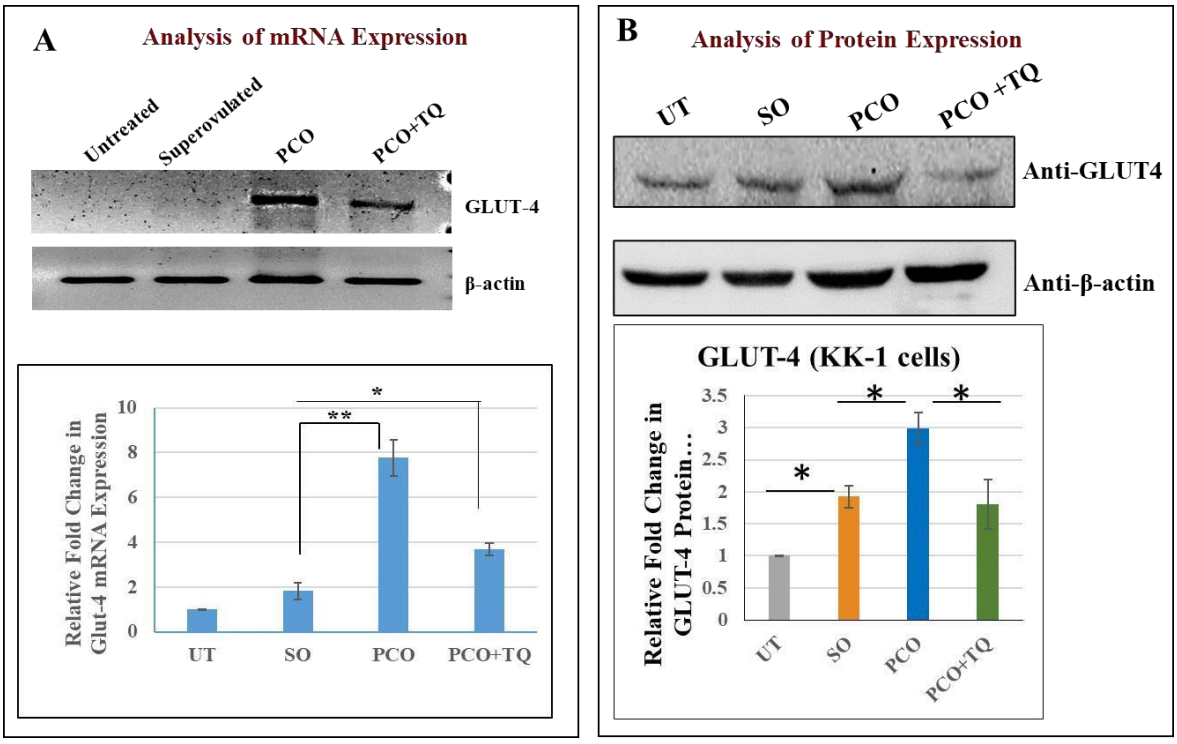

Figure 5.5A & B: GLUT-4 expression is upregulated in PCO samples in comparison to SO samples and this augmentation is reverted back by TQ treatment. (A) Semi-quantitative PCR revealed a highly significant upregulation of insulin resistance associated glucose transporter, GLUT-4 transcripts. (B) Protein

expression analysis by immunoblotting demonstrated enhanced GLUT-4 expression under PCO conditions in the KK-1 cells as evidenced from transcript analysis, indicating altered glucose uptake that is consistent with the condition of IR. Reversal of GLUT-4 levels is also evident from both the transcript and protein analysis upon TQ treatment.

Subsequently, immunofluorescence assay was performed to visualize the localization and expression of GLUT-4 in all the four experimental sets. Immunofluorescence analysis demonstrated distinctly increased expression of GLUT-4 in the PCO samples, mostly at the cell membrane (**Figure 5.5C**). This implies augmented glucose uptake under the influence of IR in PCO condition to compensate for the differential glycolysis.

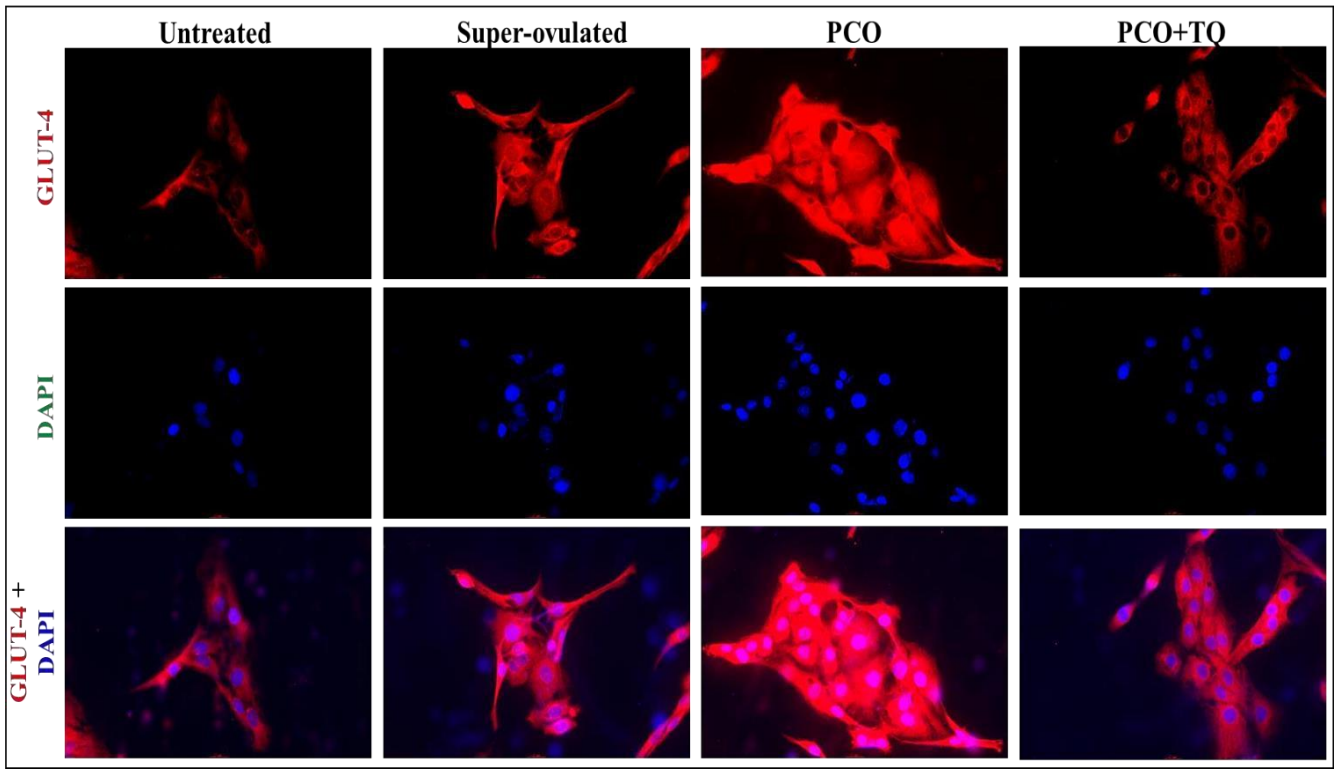

Figure 5.5C: Subcellular localization of GLUT-4 in the various experimental sets. Immunofluorescence images show GLUT-4 distribution at cell membrane. PCO samples exhibit intensified GLUT-4 fluorescence, suggesting increased recruitment of GLUT-4 which is reverted to SO levels upon pre-treatment with TQ.

5.6 Enhanced glucose uptake under PCO condition:

The evidence of elevated expression of GLUT-4 at the cell membrane of the GCs under PCO condition, suggesting increased glucose uptake; prompted us to assess the glucose uptake capacities of the experimental groups. With that aim in mind, glucose uptake assay was performed utilizing a fluorescent glucose analogue named 2-NBDG (at a final concentration of 100µM) as per protocol by both florescence microscopy [27] (**Figure**

5.6) and also fluorescence measurement by plate reader [31] (**data not shown**). In both the experiments, increased fluorescence was observed under PCO condition implying increased glucose uptake, which is concomitant with the increased GLUT-4 expression in PCO set. The fluorescence observed under the PCO+TQ set was similar to that observed under SO condition. Taken together, this data suggests that elevated GLUT-4 levels fuels heightened amount of glucose uptake by the GCs under PCO condition.

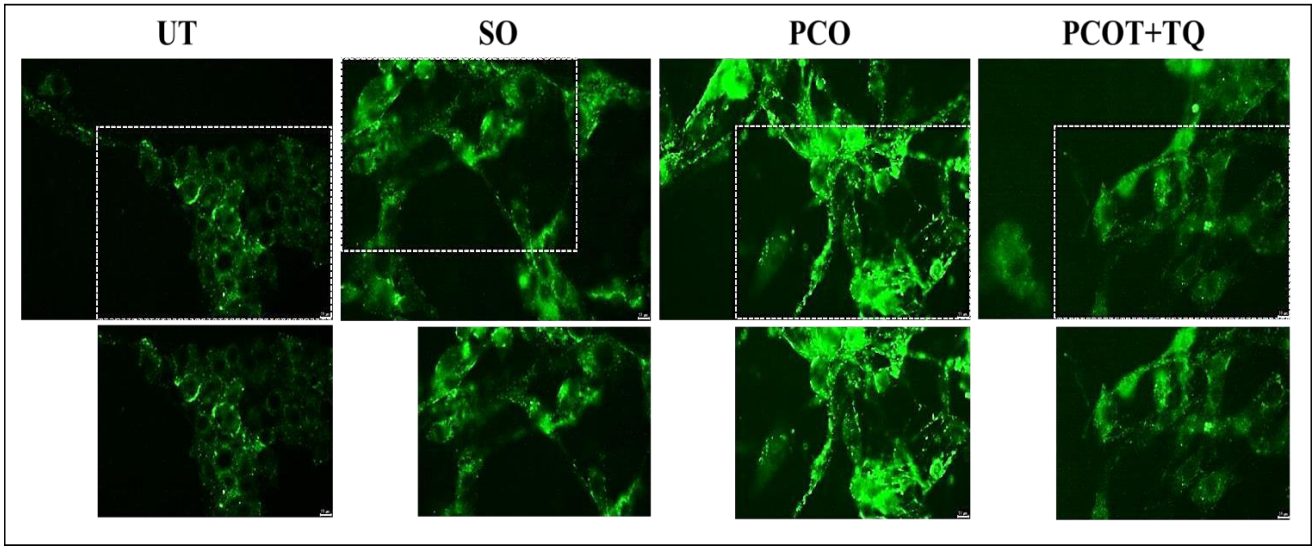

Figure 5.6: Analysis of 2-NBDG uptake in GCs through fluorescence microscopy. 2-NBDG fluorescence intensities indicate significantly increased glucose uptake under PCO conditions in comparison to SO, consistent with elevated GLUT-4 expression. Pre-treatment with TQ restores similar condition as that seen under SO condition. Scale bar represents 10µm.

Earlier studies demonstrated that an intracellular surge in glucose concentration leads to glucose induced oxidative stress [32] [33] with generation of reactive oxygen species (ROS) including nitrogen species [34] [33]. Interestingly, increased ROS has been previously reported under PCO condition both *in vitro* [35] as well as in patient samples [36]. The elevated ROS levels might be the triggering factor for increased autophagic degradation under PCO condition reported by several studies [8] [37]. Increased apoptosis has also been reported under raised concentration of glucose inside cells [33] [38]. Thus, intracellular hyperglycemic condition leading towards apoptosis or autophagic degradation might be responsible for generation of atretic follicles and impaired folliculogenesis, resulting in polycystic ovaries.

6. CONCLUSION

The observations from this study signifies a role of increased expression and nuclear localization of AR in regulating several factors associated with glycolysis under the PCO condition bringing about an impaired glucose uptake leading to impaired folliculogenesis (**Figure 6**). This might have an impact on the developing ova as the GCs are indispensable for the normal growth and function of the ova. Further the interaction of PGK1 and AR needs to be validated via co-immunoprecipitation, which can provide deeper insights about their functions.

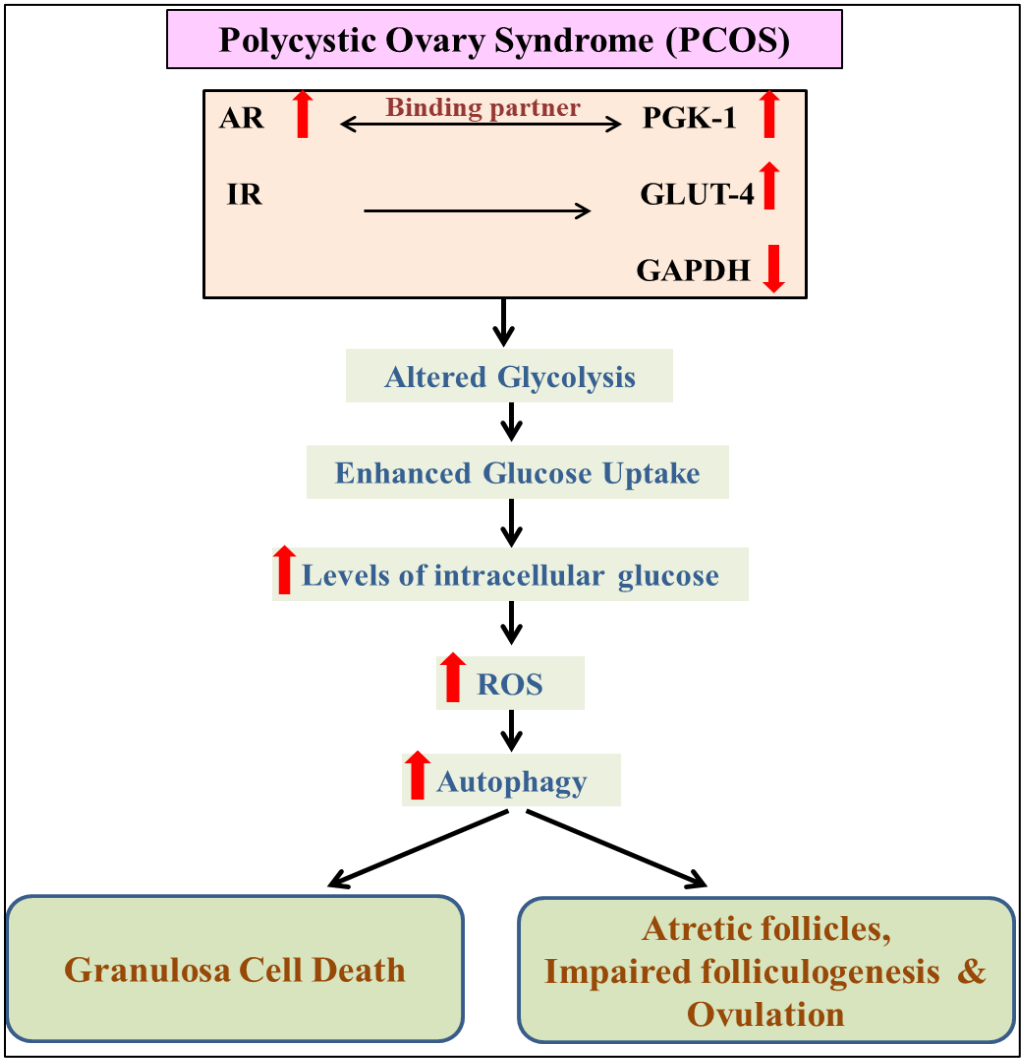

Figure 6: Flowchart describing the mechanism of impaired folliculogenesis and ovulation caused by PGK1 overexpression.

REFERENCES

1. Patel, S. Journal of Steroid Biochemistry and Molecular Biology Polycystic ovary syndrome (PCOS), an in fl ammatory , systemic , lifestyle endocrinopathy. *J. Steroid Biochem. Mol. Biol.* 0–1 (2018) doi:10.1016/j.jsbmb.2018.04.008.
2. Azziz, R. *et al.* Polycystic ovary syndrome. *Nat. Rev. Dis. Prim.* **2**, (2016).
3. Macklon, N. S. & Ph, D. Pregnancy Complications in Women with Polycystic Ovary Syndrome. **1**, 72–84 (2008).
4. Pate, K. A. & Sirmans, S. M. Epidemiology , diagnosis , and management of polycystic ovary syndrome. *Clin. Epidemiol.* **20**, 1–13 (2014).
5. Garzia, E. *et al.* Hyperandrogenism and menstrual imbalance are the best predictors of metformin response in PCOS patients. *Reprod. Biol. Endocrinol.* 1–12 (2022) doi:10.1186/s12958-021-00876-0.
6. Melnik, B. C. & Schmitz, G. Role of insulin , insulin-like growth factor-1 , hyperglycaemic food and milk consumption in the pathogenesis of acne vulgaris. 833–841 (2009) doi:10.1111/j.1600-0625.2009.00924.x.
7. Dumesic, D. A. & Richards, J. S. Ontogeny of the ovary in polycystic ovary syndrome. *Fertil. Steril.* **100**, 23–38 (2013).
8. Saha, P., Kumar, S., Datta, K. & Tyagi, R. K. Upsurge in autophagy, associated with mifepristone-treated polycystic ovarian condition, is reversed upon thymoquinone treatment. *J. Steroid Biochem. Mol. Biol.* **208**, 105823 (2021).
9. Wu, B. *et al.* Evaluation of follicular synchronization caused by estrogen administration and its reproductive outcome. *PLoS One* **10**, 1–16 (2015).
10. Zhang, C. H., Liu, X. Y. & Wang, J. Essential Role of Granulosa Cell Glucose and Lipid Metabolism on Oocytes and the Potential Metabolic Imbalance in Polycystic Ovary Syndrome. *Int. J. Mol. Sci.* **24**, (2023).
11. Kim et al. - 2014 - Original Article Correlation between Expression of Glucose Transporters in Granulosa Cells and Oocyte Quality in Wom.pdf.
12. Nicholls, C., Li, H. & Liu, J. 3rd Australia – China Biomedical Research Conference (ACBRC2011) GAPDH : A common enzyme with uncommon functions. 674–679 (2012) doi:10.1111/j.1440-1681.2011.05599.x.
13. Liu et al. - 2020 - Novel PGK1 determines SKP2-dependent AR stability and reprograms granular cell glucose metabolism facilitating ovula.pdf.
14. Vezza, T., Rocha, M. & Manuel, V. EBioMedicine PGK1-AR axis : Bene fi ts of a novel actor in PCOS pathology. *EBioMedicine* **62**, 103110 (2020).
15. Wang, T. *et al.* Differential Expression Patterns of Glycolytic Enzymes and Mitochondria-Dependent Apoptosis in PCOS Patients with Endometrial Hyperplasia , an Early Hallmark of Endometrial Cancer , In Vivo and the Impact of Metformin In Vitro. **15**, (2019).
16. Guyton & Hall, A. C. *Textbook of Medical Physiology*.
17. Sengupta, A., Narad, P., Gupta, R., Gupta, A. & Abbasi, N. Deciphering the Role of Phosphoglycerate Kinase 1 in Polycystic Ovarian Syndrome using Differential Gene Expression Analysis Approach. *Biomed. Pharmacol. J.* **16**, 773–783 (2023).
18. WHO. Plycystic Ovary Syndrome. https://www.who.int/news-room/fact-sheets/detail/polycystic-ovary-syndrome.
19. Simpson, J. L. The genetics of polycystic ovary syndrome. **18**, 707–718 (2004).
20. Havelock, J. C., Rainey, W. E. & Carr, B. R. Ovarian granulosa cell lines. *Mol. Cell. Endocrinol.* **228**, 67–78 (2004).
21. Gougeon, A. & Introduction, I. Regulation of Ovarian Follicular Development in

Primates : Facts and Hypotheses. **17**, (1996).
22. Uyar, A., Ph, D., Torrealday, S. & Seli, E. Cumulus and granulosa cell markers of oocyte and embryo quality. *Fertil. Steril.* **99**, 979–997 (2013).
23. Diaz, F. J., Wigglesworth, K. & Eppig, J. J. Oocytes are required for the preantral granulosa cell to cumulus cell transition in mice. **305**, 300–311 (2007).
24. Erickson, G. F., Hofeditz, C., Unger, M. & Allen, W. R. A Monoclonal Antibody to a Mammary Cell Line Recognizes Two Distinct Subtypes of Ovarian Granulosa. **117**, 1490–1499 (2015).
25. Thorens, B. & Mueckler, M. Glucose transporters in the 21st Century. 141–145 (2010) doi:10.1152/ajpendo.00712.2009.
26. Zhang, X. *et al.* Enhanced glycolysis in granulosa cells promotes the activation of primordial follicles through mTOR signaling. (2022) doi:10.1038/s41419-022-04541-1.
27. Yamada, K., Saito, M., Matsuoka, H. & Inagaki, N. A real-time method of imaging glucose uptake in single, living mammalian cells. *Nat. Protoc.* **2**, 753–762 (2007).
28. Yu, I., Lin, H., Sparks, J. D., Yeh, S. & Chang, C. Androgen Receptor Roles in Insulin Resistance and Obesity in Males : The Linkage of Androgen-Deprivation Therapy to Metabolic Syndrome. **63**, 3180–3188 (2014).
29. Troncoso, M. F. *et al.* Testosterone activates glucose metabolism through AMPK and androgen signaling in cardiomyocyte hypertrophy. *Biol. Res.* 1–16 (2021) doi:10.1186/s40659-021-00328-4.
30. Navarro, G., Allard, C., Xu, W., Mauvais-jarvis, F. & Orleans, N. HHS Public Access. **23**, 713–719 (2016).
31. Leira, F., Louzao, M. C., Vieites, J. M., Botana, L. M. & Vieytes, M. R. Fluorescent microplate cell assay to measure uptake and metabolism of glucose in normal human lung fibroblasts. **16**, 267–273 (2002).
32. Of, G., Oxygen, R., In, S., Cells, M. & Glucose, U. H. Reactive oxygen species as glucose signaling molecules in mesangial cells cultured under high glucose. **58**, 19–25 (2000).
33. T, D. A. A., Yaqoob, M. M. & Harwood, S. M. Mechanisms of high glucose-induced apoptosis and its relationship to diabetic complications. **16**, 705–713 (2005).
34. Thonsri, U. *et al.* High glucose-ROS conditions enhance the progression in cholangiocarcinoma via upregulation of MAN2A2 and CHD8. 254–264 (2021) doi:10.1111/cas.14719.
35. Arif, M. *et al.* Implication of thymoquinone as a remedy for polycystic ovary in rat. **0209**, (2016).
36. Dharuman, S., Kumar, S. A. & Balaji, S. K. Evaluation of Levels of Advanced Oxidative Protein Products in Patients with Polycystic Ovary Syndrome with and without Chronic Periodontitis : A Cross-Sectional Study. **16**, 55–59 (2022).
37. Li, D. *et al.* Autophagy is activated in the ovarian tissue of polycystic ovary syndrome. 1–22 (2017).
38. Yu, T., Jhun, B. S. & Yoon, Y. High-glucose stimulation increases reactive oxygen species production through the calcium and mitogen-activated protein kinase-mediated activation of mitochondrial fission. *Antioxid. Redox Signal.* **14**, 425–437 (2011).

Check Plagiarism

PLAGIARISM SCAN REPORT

Date	May 26, 2025
Exclude URL:	NO

Unique Content	**100**	Word Count	252
Plagiarized Content	**0**	Records Found	0

CONTENT CHECKED FOR PLAGIARISM:

ABSTRACT: -

Polycystic ovary syndrome (PCOS) is a multifactorial disorder characterized by hyperandrogenism, anovulation/oligo-ovulation and insulin resistance (IR). Elevated expression of the androgen receptor (AR) under PCO condition has both reproductive as well as metabolic implications. AR situationally associates with glycolytic factors like insulin like growth factor-1 (IGF-1) and phospho-glycerate kinase 1 (PGK1), leading to differential glycolysis. The granulosa cells (GCs), which surround the developing ovum are involved in a delicate play of hormones, which is dysregulated in PCOS. Utilizing an established in-vitro PCOS model comprising of mouse granulosa cell line, KK-1; our study showed that the glycolytic enzyme GAPDH was significantly downregulated while PGK1 was significantly upregulated at both the transcript and protein levels in the PCO set in comparison to the super-ovulated (SO) controls. Potential interaction between AR and PGK1 was also predicted using in silico tools, signifying AR's role in elevating PGK1 expression under PCOS. PGK1 expression was also found to be upregulated in DHT treated KK-1 cells and was reversed upon treatment with AR-blocker enzalutamide; signifying AR activation is a driving force towards upregulation of PGK1. Furthermore, immunofluorescence studies confirmed elevated expression and nuclear localization of AR and PGK1 under PCO condition. Along with that, our study showed that under PCOS condition, significant upregulation of GLUT-4 leads to increased glucose uptake in GCs and it was also demonstrated that those abnormalities seen under PCOS is reversed upon thymoquinone (TQ) treatment, thus highlighting its therapeutic potential.

Keywords: - PCOS, PGK1, GLUTs, Granulosa cells, Androgen receptor, Insulin Resistance, Glucose uptake.

MATCHED SOURCES:

Report Generated on **May 26, 2025** by https://www.check-plagiarism.com/ (https://www.check-plagiarism.com/)

Check Plagiarism

PLAGIARISM SCAN REPORT

Date	May 26, 2025
Exclude URL:	NO

Unique Content	**97**	Word Count	914
Plagiarized Content	**3**	Records Found	0

CONTENT CHECKED FOR PLAGIARISM:

1. INTRODUCTION

Polycystic ovary syndrome (PCOS) is a common endocrine disorder and gynecological ailment 1 characterized by impaired folliculogenesis and ovulatory dysfunction 2. It is also one of the primary causes of infertility among females 3. Women diagnosed with PCOS often experiences various metabolic or endocrine disruptions in which the primary defining features of PCOS are irregular menstruation, insulin resistance and hyperandrogenism respectively 2.

Insulin resistance (IR), a major symptom of PCOS, refers to a state where body cells do not uptake glucose properly and results in hyperinsulinemia and type 2 diabetes 4. IR and hyperinsulinemia can play significant role in PCOS pathogenesis by interacting with other inflammatory biomarkers 5. Also increase in insulin level in IR condition may increase the level of IGF-1 and their interaction with IGF-1 receptor has been shown to inhibit AR repressor (FOXO1) causing an upregulated AR transcription, which further worsens the PCOS condition causing hyperandrogenism 6.

Hyperandrogenism is a key hormonal imbalance that also gives rise to other PCOS symptoms like acne 6 and androgenic alopecia. Under normal physiological condition, LH stimulates the theca cells to produce androgens which is converted to estrogens by CYP19A1 (aromatase) enzyme expressed by GCs 7. Increased expression of CYP19A1 implies normal pre-ovulatory follicles but researchers have shown that in PCO condition, CYP19A1 enzyme expression and level of estradiol was strikingly downregulated than normal follicles 8 9. The hyperandrogenism in PCOS occurs due to low levels of aromatase that results into higher level of androgens and androgen receptor (AR). Previous studies demonstrated the upregulation of AR under polycystic ovarian condition using both in vitro and in vivo models 8.

In the ovaries, the process of folliculogenesis, which refers to the development of ovarian follicles into mature oocyte, along with the generation of functional granulosa cells (GCs), is tightly regulated under the influence of

FSH and hypothalamic-pituitary-ovarian axis. Proper occurrence of folliculogenesis involves two-way interaction and coordination between GCs and oocytes. GCs, situated surrounding the oocyte, are the essential elements that contribute to the healthy ovarian physiology by controlling the complex system of hormonal regulation and providing appropriate environment for follicular maturation 10. The development and maturation of oocyte requires excess amount of energy which is primarily fueled by glucose through glycolytic pathway, the most widely available energy substrate in the body 11. GCs uptake large amount of glucose with the help of glucose transporter proteins (GLUTs) on their surface, and produce glycolytic metabolites such as pyruvate and lactate because of high enzymatic activity followed by supplying pyruvate and lactate to the oocyte which is not efficient in conducting glycolysis due to the lack of glucose transporter proteins (GLUTs) on their surface and glycolytic enzymes 10. This phenomenon is mediated by pyruvate dehydrogenase kinase (PDK) expressed by cumulus GCs that inhibits pyruvate dehydrogenase (PDH) and prevents the entry of pyruvate in TCA cycle within GCs 10. The GCs thus fulfills the energy needs of the oocyte through generation of increased levels of pyruvate and lactate (Figure 1).

Figure 1: Interplay between granulosa cells and oocyte.

GLUTs are specialized kind of proteins present on the surface of GCs that assists in effective glucose transportations across cell membrane 11. Among various types of GLUTs, GLUT-1 is constitutively expressed while GLUT-4 is differentially expressed 11. Under normal physiology, GLUT-1 is primarily present on the surface of GCs. But in PCOS condition owing to insulin resistance, GLUT-4 is upregulated and GLUT-1 is downregulated in human GCs 11. Efficient glycolysis for supporting folliculogenesis relies heavily on two important enzymes namely glyceraldehyde-3-phosphate dehydrogenase (GAPDH) and phosphoglycerate kinase-1 (PGK1) 12 13. GAPDH catalyzes the sixth step in glycolysis by converting glyceraldehyde-3-phosphate (GAP) into 1,3-bisphosphoglycerate (1,3-bisPG) in the presence of NAD+ and inorganic phosphate, which is the first redox reaction of glycolysis 12 and also PGK1 catalyzes the first ATP producing step of glycolysis by converting 1,3-bisPG into 3-phophoglycerate. PGK1 plays important role in driving the glycolytic pathway forward in GCs and thus optimally supplying energy for proper folliculogenesis 11. It is hypothesized that PGK1 might have positive correlation with AR 13. PGK1 is thought to interact with AR present in GCs 14. Another study has demonstrated that in the luteinized GCs of PCOS patients and ovarian tissues of PCOS like mouse models, PGK1 level is increased which further exacerbates the PCOS like symptoms in mouse models. However, the exact mechanism through which PGK1 controls the glucose metabolism in GCs and contributes to IR and other metabolic disorders, is still unclear 14. Apart from this, differential expression of GLUTs and glycolytic enzymes has been observed in endometrial tissues of PCOS patients 15 but there are no studies about expression profiles of the GLUTs and glycolytic enzymes in local ovarian tissues and GCs.

Since there are various studies about differential expressions of glycolytic enzymes and GLUTs only in

endometrial tissues, the present study intends to inspect if there are alterations of the same at the local ovarian tissues. This study utilizes already established in vitro PCOS models which were generated using murine GC line, named KK-1. Several studies have been performed using KK-1 as a model. This cell line is an excellent system for studies because it exhibits the characteristics of a typical GC, e.g. responsiveness to gonadotropins and inhibin expression. In addition, KK-1 cells can be easily maintained in culture and transfected with high efficiency. Studies on the RU486 treated hormone primed ovarian granulosa cell line KK-1, displayed some molecular features similar to what is observed in GCs from PCOS patients 8.

MATCHED SOURCES:

Upsurge in autophagy, associated with mifepristone-treated ...

https://www.sciencedirect.com/science/article/abs/pii/S09600....
(https://www.sciencedirect.com/science/article/abs/pii/S0960076021000169)

Report Generated on **May 26, 2025** by https://www.check-plagiarism.com/ (https://www.check-plagiarism.com/)

Check Plagiarism

PLAGIARISM SCAN REPORT

Date	May 26, 2025
Exclude URL:	NO

Unique Content	**97**	Word Count	947
Plagiarized Content	**3**	Records Found	0

CONTENT CHECKED FOR PLAGIARISM:

2. REVIEW OF LITERATURE

During the active reproductive years in women, a recurring pattern of hormonal shifts occurs each month, bringing about a sequence of functional changes in the ovaries and other reproductive organs. This regular biological rhythm, driven by the rise and fall of female sex hormones, governs the preparation for potential fertility and is formally recognized as the female monthly reproductive cycle, commonly known as the menstrual cycle 16. The process consists of strict hormonal control which is regulated by hypothalamus. The hypothalamus produces GnRH hormone which stimulates anterior pituitary gland to secrete two important gonadotropins - FSH (follicle stimulating hormone) and LH (luteinizing hormone). FSH and LH stimulate the growth and development of Graafian follicles in ovary and leads to ovulation and estrogen production.

The growth of follicles from the primordial follicles to primary oocytes via formation of oogonial mother cell (2n) in human embryonic ovaries takes approx. 6.5 months. During the last 2 weeks, formation of antral follicles occurs which is characterized by slower oocyte growth, extracellular fluid formation, granulosa cell (GCs) differentiation into mural and cumulus phenotypes, and selection of a dominant follicle. Early antral follicles in human are under the influence of and are highly responsive to FSH. Theca cells, under stimulation by LH, produce androgens, which subsequently diffuse into adjacent GCs. In GCs, FSH promotes the expression of the enzyme CYP19A1 (aromatase), which catalyzes the conversion of androgens to estrogens 7. Increased expression of CYP19A1 within GCs is recognized as a characteristic marker of a normal pre-ovulatory follicle 8. After ovulation, LH promotes differentiation of Graafian follicle into corpus luteum which produces progesterone hormone. Increased levels of estrogen at mid-cycle give positive feedback to anterior pituitary to produce more LH. Finally increased level of estrogen and progesterone hormone gives negative feedback to anterior pituitary and to stop FSH, LH production and hypothalamus to stop GnRH production. But this hormonal control may get disrupted by poor lifestyle, diet or sometimes by environmental factors that gives rise to most common metabolic, endocrine

disorder in female before menopause termed as polycystic ovarian syndrome (PCOS) 17.

Polycystic ovarian syndrome (PCOS) is the current epidemic that impacts an estimated 6-13% women during their reproductive years and up to 70%fected women remain undiagnosed worldwide 18. PCOS is a polygenic, polyfactorial, systemic, inflammatory, dysregulated steroid state and autoimmune disease. Even though the etiology of this endocrinopathy is not clearly understood 15 or can't be cured, but symptoms still can be improved by lifestyle changes, medication or fertility treatments. The most prominent manifestations of PCOS include hyperandrogenism and insulin resistance (IR) 19. Women with PCOS often suffer with a cluster of symptoms such as irregular or absent menstrual cycle, ovulatory dysfunction/chronic anovulation 20, hirsutism, obesity, type 2 diabetes, gestational diabetes, metabolic syndrome, hypertension 4, multiple fluid filled cysts, androgenic alopecia 17. The most defining feature of PCOS is low level of CYP19A1 (aromatase) 9 and IR 20. Researches have shown that in PCOS condition, the concentration of estradiol and CYP19A1 is prominently lower than that of normal follicles 9. Apart from these, insulin resistance (IR) is a major symptom of PCOS. IR refers to a state where the body cells do not respond optimally to normal insulin levels. It results in hyperinsulinemia or excessive insulin in blood stream, and can lead to diabetes mellitus. IR and hyperinsulinemia, along with inflammatory conditions in PCOS can promote abnormal androgen production, disrupted normal folliculogenesis and irregular menstruation, thus playing significant role in PCOS pathogenesis. The hyperandrogenism seen under PCOS condition can be attributed to high levels of androgens due to low levels of aromatase and also high levels of AR (androgen receptor), as has been previously observed under both in vivo and in vitro condition 8. Along with it, elevated level of insulin upon IR may increase the level of free insulin-like growth factor (IGF-1) and together they interact with a receptor, IGF-1R. This inhibits AR repressor (FOXO1) causing an augmented AR transcriptional activity 6, thus aggravating the symptoms associated with hyperandrogenism.

GCs, often overshadowed by their oocyte counterpart, are inevitable architects of ovarian physiology, coordinating an intricate network of hormonal signalling, cellular differentiation, and follicular maturation that forms the foundation of female fertility 10. Development of functional GCs can be traced back to the incidence of folliculogenesis that begins in a 4 months old female foetus where primordial follicles start to accumulate in the foetal ovary and generate the resting follicle pool (RF) 21. Primordial follicles have simple structure containing oocyte arrested at prophase 1 and a single layer of squamous GCs around it, confined under basement membrane 22. In subsequent stages of folliculogenesis, the GCs become cuboidal and gets differentiated into – mural GCs, located around the oocyte; and cumulus GCs, facing the antrum follicle 23. Cumulus granulosa cells (CCs) further differentiate into corona radiata cells, which can support and guide sperm into the egg during fertilization 10. In spite of the facts the both MGCs and CCs have arisen from the same progenitor precursor cells, MGCs and CCs have significant functional differences 24. During the early stages of oocyte development, the MGCs synthesize estrogen (estradiol) for the development of female secondary sexual characteristics and

regulation of reproductive cycle 20. CCs are primarily responsible for providing environmental support for oocyte maturation. They establish gap junctions which allow oocytes through and permit the two-way conduction of information between GCs, enable metabolism and nutrient exchange 10. Together the GCs give metabolic support to the developing oocyte by acquiring glucose from the surrounding tissues via the GLUTs, present on their cellular membrane, resulting in pyruvate and lactate production via glycolysis. This is the primary source of energy for proper folliculogenesis 11.

MATCHED SOURCES:

Polycystic ovary syndrome (PCOS), an inflammatory, systemic ...

https://pubmed.ncbi.nlm.nih.gov/29678491/ (https://pubmed.ncbi.nlm.nih.gov/29678491/)

Essential Role of Granulosa Cell Glucose and Lipid Metabolism on ...

https://www.mdpi.com/1422-0067/24/22/16247 (https://www.mdpi.com/1422-0067/24/22/16247)

Report Generated on **May 26, 2025** by https://www.check-plagiarism.com/ (https://www.check-plagiarism.com/)

Check Plagiarism

PLAGIARISM SCAN REPORT

Date	May 26, 2025
Exclude URL:	NO

Unique Content	**100**	Word Count	667
Plagiarized Content	**0**	Records Found	0

CONTENT CHECKED FOR PLAGIARISM:

Since glucose is a key fuel and an important metabolic substrate that regulates gene transcription, enzyme activity, hormone se¬cretion and gluco-regulatory neuron activity in mammals 11, any change in its regulation may have altered metabolic implication. It is important to note that differential glycolysis is one of the major consequences of PCOS. Differential expression of glycolytic enzymes in endometrial tissues affected by PCOS has been observed 15 but evidences supporting the same in case of local ovarian level or GCs surrounding the oocyte are yet to be researched.

For glycolysis in the GCs to occur properly and support folliculogenesis under normal physiologic condition, two most important glycolytic enzymes that are crucial, are glyceraldehyde-3-phosphate dehydrogenase (GAPDH) and phosphoglycerate kinase 1 (PGK1) 12. In glycolysis, GAPDH catalyzes the conversion of glyceraldehyde-3-phosphate (GAP) into 1,3-bisphosphoglycerate (1,3-bis PG). GAPDH catalyzes the first redox reaction in glycolysis by producing NADH by reducing NAD+ and oxidizing GAP 12. On the other hand, PGK1 catalyzes the first ATP producing reaction in glycolysis by conversion of 1,3-bis PG into 3-phosphoglycerate and prevents the pathway from going backward, thus optimally regulates the glucose metabolism in GCs and supplies energy for folliculogenesis 11. Further, PGK1 also has vital interactions with AR 13. During folliculogenesis, AR is very important for follicular growth which is mostly expressed on the surface of ovarian GCs 15. PGK1 is known to regulate glucose metabolism in coordination with AR 14. In another study, an elevated abundance of PGK1 has been observed in luteinized GCs from PCOS patients as well as in ovarian tissues of PCOS-like mouse models, regulated glucose metabolism in them and further degrades the PCOS-like symptoms in mouse. It has been hypothesized that there might be a positive correlation between PGK1 and AR 13. However, the precise mechanisms through which PGK1 governs glucose metabolism in GCs, contributing to IR and other metabolic complications associated with PCOS, remain largely elusive 14.

As mentioned earlier, besides serving as a vital energy force, glucose is also a critical metabolic substrate that

influences gene expression, modulates enzymatic functions, governs hormone release and impacts the activity of gluco-regulatory neurones in mammals 25. In mammalian cells, the movement of glucose across the plasma membrane is mediated by a specialized family of proteins known as glucose transporters (GLUTs), which facilitate its efficient transport 11. Previous studies showed that expression of GLUTs changes in PCOS condition. Under normal physiology, GLUT-1 is predominantly present on the surface of GCs. But in PCOS condition, GLUT-4 is upregulated and GLUT-1 is downregulated 11. As a result it can be hypothesized that glucose uptake will also be increased. Nonetheless, the expression profiles and functional roles of the more recently identified GLUT isoforms remain comparatively underexplored within ovarian tissues. Researchers have shown that in mouse, the transition of primordial to primary follicles is accompanied by increased energy requirement or glycolysis in GCs along with upregulation of GLUT-4 (glucose transporter-4) and glycolysis rate-limiting enzymes such as hexokinase 1 (HK1), phosphofructokinase (PFKL) and pyruvate kinase M2 (PKM2). The mTOR signaling is crucial here to provide enough energy for increased metabolism and stimulate folliculogenesis 26. Also, in PCOS patients, GLUT-4 protein expression is found to be decreased in adipocytes while GLUT-1 expression is increased in skeletal muscles. Reduced expression of GLUT-4 is also found due to reduced level of estrogen in uterus 11.

Previous studies by Saha et al and group (2021) have shown that upregulated levels of AR and downregulated levels of CYP19A1 (aromatase) are reverted upon treating GCs or PCO rats with a herbal drug named as thymoquinone (TQ) 8. Taken together, these considerations form the basis for the present study, which seeks to investigate alterations in glycolytic enzymes and GLUT expression at the local ovarian level under polycystic ovarian condition utilizing an established PCOS model 8 based on the murine granulosa cell line KK-1. This study can potentially offer deeper insights into cellular metabolic disruptions that contribute to the onset of PCOS, and the potential therapeutic effect of TQ on the same if any.

MATCHED SOURCES:

Report Generated on **May 26, 2025** by https://www.check-plagiarism.com/ (https://www.check-plagiarism.com/)

Check Plagiarism

PLAGIARISM SCAN REPORT

Date	May 26, 2025
Exclude URL:	NO

Unique Content	**100**	Word Count	366
Plagiarized Content	**0**	Records Found	0

CONTENT CHECKED FOR PLAGIARISM:

3. AIMS & OBJECTIVES

As evident from the existing literature, women with PCOS exhibit lower CYP19A1 (aromatase) expression, elevated androgens and AR ensuing activated androgen-AR signaling implicated in impaired folliculogenesis that causes chronic anovulation and a chronic accumulation of androgens within the female body leading to hyperandrogenism 8. The normal development of follicles and the consequential maturation of oocyte depends mainly on the uptake of glucose from the surrounding tissues by GCs via GLUTs on their cell membrane. Interestingly, AR-androgen axis under homeostasis has been implicated to regulate glycolysis.

Thus, we hypothesize that: “Elevated AR expression under polycystic ovarian condition dysregulates glycolysis resulting in impaired folliculogenesis”.

The objective of the present study is as follows:

“To elucidate the effect of elevated AR expression on glycolytic factors and downstream targets with special emphasis on key glycolytic enzyme PGK1 under PCO condition”.

4. MATERIALS AND METHODS

4.1 Materials

4.1.1 Chemicals and Kits used:

Regular lab reagents were either purchased from HiMedia Laboratory Pvt Ltd. (Maharashtra, India) or Sisco Research Laboratories Pvt Ltd. (Maharashtra, India).

PureZol, Biorad was used for RNA extraction.

iSCRIPTTM RT-PCR Kit with SYBR Green from BIO-RAD was used for cDNA preparation and PCR amplification.

Secondary antibodies were obtained from Sigma Aldrich Chemicals Pvt. Ltd. (USA) and Cell Signaling Tech. (USA), AbClonal.

Water used for preparing buffers, reagents was either autoclaved triple distilled or Milli Q (obtained from water purification system, Millipore, MA, USA).

Cell culture plastic wares were obtained from Corning-Costar Inc. (Sigma/Merck USA).

PVDF membranes for filtering media and 0.22 µM membrane filters were obtained from Merck Millipore (MA, USA).

Filtration unit and isopropanol cryobox were purchased from Tarsons (India).

2-NBDG dye [2-(N-(7-Nitrobenz-2-oxa-1,3-diazol-4-yl)Amino)2 deoxyglucose] was purchased from MedChemExpress (MCE), Cat. No.: HY-116215

DHT (Dihydrotestosterone) was purchased from Supelco.

Enzalutamide was purchased from MedChemExpress (MCE), Cat. No.: HY-70002

4.1.2 Equipment used:

Colibri nanodrop instrument was used for estimating RNA concentration and purity.

First strand synthesis (cDNA preparation) was performed in Biorad S1000 Thermal Cycler.

qRT-PCR was performed using CFX connect Real-Time Detection System.

Fluorescence microscope Leica DM6 B by Leica Microsystems CMS GmBH, Germany.

BIORAD ChemidocTM MP Imaging System.

MATCHED SOURCES:

Report Generated on **May 26, 2025** by https://www.check-plagiarism.com/ (https://www.check-plagiarism.com/)

Check Plagiarism

PLAGIARISM SCAN REPORT

Date	May 26, 2025
Exclude URL:	NO

Unique Content	**97**	Word Count	900
Plagiarized Content	**3**	Records Found	0

CONTENT CHECKED FOR PLAGIARISM:

Methods

4.2.1 Mammalian cell culture:

(A) Maintenance of murine granulosa cell line, KK-1:

The KK-1 granulosa cell line was developed in the laboratory of Dr. Ilpo Huhtaniemi, University of Turku, Finland and was procured from Dr. Nafis Rahman. Cells were maintained in high glucose DMEM (Dulbecco's Modified Eagle's Medium), containing 4.5 gm/L glucose. The media was supplemented with 10�S (Origin South America, PAN-Biotech, Germany), 50 IU/mL penicillin, 50 µg/mL streptomycin and 0.25 µg/mL amphotericin B in tissue culture plates. The cultures were grown at 37°C in a humidified atmosphere with 5% CO2 and 95% air. The cells were routinely passaged to maintain a monolayer culture by detaching from the plastic surfaces of cell culture plates by trypsinization. Cells were also sub-cultured regularly.

(B) Creation of hormone primed in vitro models using KK-1 cell line (UT, SO, PCO, TQ):

The hormone treated in vitro models of super-ovulated (SO), polycystic ovary (PCO)/anovulatory condition and thymoquinone (TQ) treated PCO models were created as per established protocol 8. First the cells were seeded on 100 mm cell culture plates and those plates undergone media change after 6 hours of seeding (0 hour). After 40 hour of cell growth, cells were treated with hCG (10 IU/mL) i.e. hormone primed in order to mimic the physiological condition and these are termed as SO. For generating the PCO experimental set, the KK-1 cells were treated with both hCG and an anti-progestogen drug mifepristone, also known as RU486 (10 µM or 50 µM), at 40 hour of growth. For the thymoquinone (TQ) treated PCO model, the cell were treated with TQ (10 µM) beforehand, at 36h of growth. Next it was treated with hCG and RU486 at 40 h of growth. All those cells were harvested after 8 hours of i.e. 48 hours of growth. Untreated (UT) KK-1 cells were grown for 48 hours for using as a control (Figure 4.2A).

Figure 4.2A: Generation of different experimental sets (Control, Super-ovulated, PCO induced and TQ pre-

treated) utilizing KK-1 cell line

(C) Treatment of cells with dihydrotestosterone (DHT):

Dihydrotestosterone (DHT) is a potent androgen that binds to the androgen receptor (AR) and activates it. Once activated, AR translocates to the nucleus and acts as a transcription factor to regulate various gene expressions governed by AR itself. Enzalutamide is a non-steroidal, anti-androgen that competes with DHT to bind to AR. Upon binding, it prevents AR activation, inhibits its nuclear translocation and blocks AR-mediated transcription of androgen-responsive genes. In order to examine any change in expression of PGK1 upon AR activation, KK-1 cells were treated with DHT, a known agonist of AR signaling. Cells were seeded on four 100 mm cell culture plates and they were treated as follows – VT (vehicle treated), KK-1+DHT (dihydrotestosterone), KK-1+AR Blocker (enzalutamide) and KK-1+DHT+enzalutamide. The concentration of DHT and enzalumamide used for treatment are 50nM and 5µM respectively. The treatment was given for a period of 24h and subsequently the cells from all four experimental sets were harvested for protein sample preparation.

4.2.2 RNA extraction, estimation & purity checking:

All the four cell samples (UT, SO, PCO, TQ) were treated with TRIzol reagent and taken into fresh 4 microcentrifuge tubes and were centrifuged for 2 minutes at 13000 rpm at 4°C. After centrifugation, the supernatant was collected and put into fresh four microcentrifuge tubes and labeled accordingly. Next 0.2 ml (200 µl) chloroform ($CHCl_3$) was added to each tube and contents were mixed thoroughly by rigorously shaking and inverting the tubes for 30 seconds (tubes should be vortex to avoid RNA degradation into pieces) and incubated at room temperature (RT) for 5 minutes and mixing periodically. Centrifuge each tube at 12000 g for 15 minutes for phase separation. The aqueous phases from each tube were carefully transferred to fresh microcentrifuge tubes without disturbing the interphase. Next 0.5 ml (500 µl) isopropanol was added to each tube followed by thorough mixing and incubate at RT for 5min. The tubes were centrifuged at 12000 g for 10 min at 4°C. After centrifugation, supernatant was discarded and pellet was resuspended with 1 ml of 75% ethanol. Samples were vortexed and centrifuged 7500 g for 5 minutes at 4°C and the supernatant was discarded, pellet was allowed to air dry completely by inverting the tubes keeping lids open on a clean, dry piece of tissue paper. After drying the pellet, it was resuspended in nuclease free water (NFW), properly mixed by pipetting. This newly extracted RNA samples were kept at RT and stored in ice before estimation. The absorbances of the samples were measured at 260 nm and concentration (ng/µl) using Colibri Nanodrop instrument. Along with that, the purity of prepared samples was checked by measuring the absorbance ratios A260/280 and A260/230. cDNA was also prepared according to the calculations in the below table. Remaining RNA samples were stored at -80°C.

RNA Quantification

Sample OD 260/280 OD 260 Concentration (ng/µl) Volume required for 5 µg (5000/conc.)

UT 1.92 16.47 658.91 7.58

SO 1.98 12.31 492.57 10.15

PCO 1.98 8.78 351.10 14.24

TQ 1.89 27.40 1096.06 4.56

Table 1: Table showing Nanodrop readings for RNA concentration, A260/280 reading and volume (µl) required for 1 µg of RNA from ovary samples to be used for cDNA preparation.

Sample RNA NFW Mastermix (reverse transcriptase+buffer)

UT 7.58 7.42 5

SO 10.15 4.85 5

PCO 14.24 0.76 5

TQ 4.56 10.44 5

Table 2: Table showing the exact volume of reagents for cDNA preparation reaction.

MATCHED SOURCES:

Upsurge in autophagy, associated with mifepristone-treated polycystic ...

https://www.sciencedirect.com/science/article/pii/S096007602....
(https://www.sciencedirect.com/science/article/pii/S0960076021000169)

Comparative evaluation of 19 reverse transcription loop-mediated ...

https://www.nature.com/articles/s41598-020-80314-0 (https://www.nature.com/articles/s41598-020-80314-0)

Report Generated on **May 26, 2025** by https://www.check-plagiarism.com/ (https://www.check-plagiarism.com/)

Check Plagiarism

PLAGIARISM SCAN REPORT

Date	May 26, 2025
Exclude URL:	NO

Unique Content	**95**	Word Count	874
Plagiarized Content	**5**	Records Found	0

CONTENT CHECKED FOR PLAGIARISM:

4 Protein sample preparation from experimental set cell lysates and concentration estimation:

The experimental sets of cells were grown in 100 mm plates, and treatment was given as per the lab protocol. For each set, 3 confluent 100 mm cell culture plates were taken and the existing exhausted media was discarded from the plates. Then each plate was washed with 1X PBS. To the plates, 1 ml trypsin was added and incubated at 37°C, 5% CO2 for 2-3 minutes. After 2-3 minutes of incubation, 1 ml fresh DMEM containing 10�S was added to the plates to make a uniform cell suspension. The cell suspension were taken in 15 ml falcons and centrifuged at 700 rpm for 5 minutes and the supernatant was discarded. Then 200 µl 1X PBS was added to the cell pellet obtained and it was resuspended by pipetting to wash out the residual DMEM media. The suspension was then collected in microcentrifuge tubes and centrifuged at 800 rpm for 5 minutes. The supernatant was discarded and the pellet was stored at -20°C.

The cell pellets were treated with RIPA buffer and kept in icebox. Next, they were slowly rocked until the mixture turns transparent. The cells were centrifuged at 13000 rpm for 15 minutes at 4°C. Fresh microcentrifuge tubes were prepared and labeled in which the supernatant was collected. Similarly, protein was extracted from DHT treated samples. Then protein estimation assay was performed using Bradford reagent. Protein content of each sample was estimated using standard Bradford method with known standard curve of bovine serum albumin (BSA). The concentration of the samples was determined from the equation received from the standard curve. Following protein quantification, one-fourth the volume of 5X SDS sample buffer was added to each microcentrifuge tube containing the respective samples. The mixtures were then incubated in a dry bath at 95°C for 15 minutes to ensure protein denaturation, promptly chilled on ice to stabilize the denatured proteins, and centrifuged at 13,000 rpm for 15 minutes at 4°C. The resulting supernatants were carefully collected and preserved at −20°C for further analysis.

Samples Average OD at 595 nm

Blank 0

BSA 2 0.208667

BSA 5 0.369667

BSA 10 0.427333667

BSA 15 0.610333667

BSA 20 0.673000333

UT 0.67

SO 0.67

PCO 0.70

TQ 0.69

Table 4: Table showing average OD at 595 nm after subtracting the Blank reading by Bradford Assay

Figure 4.2C: BSA standard Graph obtained from BSA known Concentration

4.2.5 Sodium dodecyl sulfate polyacrylamide gel electrophoresis:

Linear slab gel electrophoresis under denaturing condition was performed to separate the protein bands. Suitable volume of samples was loaded into the respective wells of the gel from each of the samples – UT, SO, PCO, TQ. Along with that, appropriate amount of protein ladder was also loaded. The proteins were stacked at pH 6.8 in 4% stacking gel containing 4�rylamide, 0.106% N, N'-methylene bis-acrylamide, 0.125 M Tris-HCl, 0.01% TEMED and 0.1% ammonium per sulphate (APS). The resolving gel was 12.5% and had pH of 8.8, consisting of 12.5�rylamide, 0.33% N, N'-methylene bis-acrylamide, 0.375 M tris-HCl, 0.01% TEMED and 0.1% APS. Proteins were electrophoresed in running buffer of pH 8.3, containing 0.025 M Tris-base, 0.192 M glycine and 0.1% SDS. The voltage was kept at 60 V when the bands were in stacking gel and increased to 120 V when bands reached the resolving gel. This voltage was maintained throughout the run.

4.2.6 Western blotting:

After electrophoretically separating the proteins, the bands were transferred onto a PVDF membrane, which was first blocked for 1 hour with 3% BSA solution dissolved in PBS. Then the blot was washed with PBST (0.05% tween 20 dissolved in PBS) for 5 minutes on fast rocker. Next the blot was incubated with primary antibody (anti-rabbit-GLUT-1, anti-rabbit-GLUT-4, anti-rabbit-PGK1, anti-rabbit-β actin) dissolved in 1.5% BSA solution overnight at 4°C on slow rocker. Then the blots were washed with PBST thrice, each for 15min on fast rocker. Next the blot was incubated with secondary antibody (HRP or AP conjugated secondary antibodies were used that were either raised in mice or rabbit, as per requirement) dissolved in 1.5% BSA solution at room temperature for 1 hour on slow rocker followed by 3 PBST washes, each for 15 minutes. Next the blots were developed by using appropriate substrates and their respective protocols.

4.2.7 Detection of protein by enhanced chemiluminescence (ECL) or colorimetry:

For detecting the blots with immune complexes containing HRP tagged secondary antibodies, enhanced chemiluminescence was used. The blots were treated with ECL reagents – 22 µl p-coumaric acid (90mM), 50 µl luminol (250 mM) and 3 µl (30%) H_2O_2 dissolved in 10ml Tris- buffer (pH 8.5). For detection of protein bands, an instrument called BIORAD ChemiDocTM MP Imaging System was used and chemiluminescence was captured. For detecting the blots with immune complexes containing alkaline phosphatase (AP) tagged secondary antibodies, colorimetric detection protocol was used. AP reaction mix was prepared by dissolving 66 µl NBT (50 mg/ml) and 33 µl BCIP (50 mg/ml) into 10 ml AP buffer (pH 9.5). Next the AP reaction mix was added to the boxes containing the blots and covered fully with aluminum foil as these are light sensitive and optimal reaction needs dark environment. Blots were incubated on slow rocker until bands are visible.

MATCHED SOURCES:

eprints.whiterose.ac.uk › id › documentStructures of α-galactosaminidases from the CAZy GH114 family and...

https://eprints.whiterose.ac.uk/id/document/3494040/ (https://eprints.whiterose.ac.uk/id/document/3494040/)

Protein Extraction - protocols.io

https://www.protocols.io/view/protein-extraction-261geoz9yl4.....(https://www.protocols.io/view/protein-extraction-261geoz9yl47/v1)

Report Generated on **May 26, 2025** by https://www.check-plagiarism.com/ (https://www.check-plagiarism.com/)

Check Plagiarism

PLAGIARISM SCAN REPORT

Date	May 27, 2025
Exclude URL:	NO

Unique Content	**100**	Word Count	661
Plagiarized Content	**0**	Records Found	0

CONTENT CHECKED FOR PLAGIARISM:

Immunofluorescence studies:

The cells were seeded onto the surface of coverslips, kept in a 12 well. Then the media was gently aspirated out of the wells and the wells were washed with 1X PBS. The cells were fixed with chilled methanol and stored at -80°C. Next day, the fixed cells were observed under microscope and the coverslips were transformed to another fresh 12 well plate where in each well 1 ml paraformaldehyde (PFA) was added. Incubate at 37°C for 15 minutes. Next PFA was removed by adding 1X PBS to the wells and washed by shaking with palms until the smell of PFA is faded. Next, 1 ml Glycine was added into each well and incubated at 37°C for 5 minutes followed by washing with PBS. Next, 1 ml Triton X100 was added to create pores in the cell membrane so that cells become receptive to antibodies. It was incubated at 37°C for 1 min followed by removal of the Triton X 100 with PBS wash. After that, 12 parafilm squares were cut in the size of the wells and those squares were placed on the lid. On each square, 50 µl blocking solution (3% BSA+PBS) was placed and the coverslips were placed with the help of needle and forceps such that the cell side faces the blocking solution. The lid was incubated in a moist chamber for 1 hour at 37°C followed by washing with PBS. Next on each strip, 50 µl primary antibody (anti-mouse-AR and anti-rabbit-PGK1 in one set and in another set anti-rabbit-GLUT-4) solutions were added and coverslips were put back in previous manner. It was incubated overnight at 4°C. Next day, coverslips were washed with 1X PBS thrice each for 10 minutes. The coverslips were incubated with 50 µl fluorescent tagged secondary antibody solution (anti-rabbit-green, anti-mouse-red in case of co-localization studies between AR and PGK1, and anti-rabbit-red in case of GLUT-4) in a moist chamber at 37°C for an hour followed by washing with 1X PBS twice for 20 minutes. Meanwhile, the nuclei were stained with DAPI solution. Next, on a clean slide approximately 20 µl of 50% glycerol was added and coverslips were carefully placed on slide with cell facing the glycerol. Coverslips were sealed with clear nail polish and examined under microscope.

4.2.9 Glucose uptake assay using 2-NBDG:

Glucose uptake in live cells was assessed using the fluorescent glucose analog 2-NBDG [2-(N-(7-Nitrobenz-2-oxa-1,3-diazol-4-yl)Amino)-2-deoxyglucose]; following previously established protocols 27 with minor modifications. Cells were seeded onto coverslips in 12 well plates (Corning) and cultured to ~60% confluence under standard conditions (37°C, 5% CO_2). The cells were pre-treated with TQ (10 µM) at 36 h of growth. After 40 h of growth, cells were treated with hCG (10 IU/ml) and RU486 (10 µM or 50 µM), to create SO and PCO models, as per the established protocol 8 described earlier. At 48 h of growth, media was discarded and cells were washed with PBS. Cells were incubated with PBS at 37°C for 10 minutes. Next on clean slides, 50 µl of 2-NBDG (100 µM) was dispensed and cover slips were placed with cell sides facing the 2-NBDG. Cells were incubated for 15 minutes in dark. After incubation, coverslips were washed with PBS to remove unincorporated dye. The washed coverslips were put back on the respective slides and sealed with clear nail polish. Next, they were immediately subjected to live-cell fluorescence imaging (excitation: 467 nm, emission: 538 nm).

Figure 4.2D: Image showing the working principle of 2-NBDG

(Image source: https://www.dojindo.com/JP-EN/products/UP02/img/up02_principal.png)

4.2.10 Statistical analysis:

ImageJ software was used to analyze band intensities of the immunoblots and after normalization with the loading controls, relative fold changes were calculated accordingly. All data are represented as mean ± SD of observations from different experiments in triplicates (n=3). Unpaired students t- test was performed using GraphPad, Quickcalcs software. Difference at a level of* $p < 0.05$,** $p < 0.01$ (or as indicated in the Figures) between groups are considered statistically significant.

MATCHED SOURCES:

Report Generated on **May 27, 2025** by https://www.check-plagiarism.com/ (https://www.check-plagiarism.com/)

Check Plagiarism

PLAGIARISM SCAN REPORT

Date	May 27, 2025
Exclude URL:	NO

Unique Content	**100**	Word Count	882
Plagiarized Content	**0**	Records Found	0

CONTENT CHECKED FOR PLAGIARISM:

5. RESULTS AND DISCUSSION

5.1 Differential expression of the glycolytic enzymes GAPDH and PGK1 under PCO condition:

Androgen-AR axis has been implicated to play a crucial role in tissue-specific regulation of glucose metabolism 28 which includes cardiomyocytes 29, skeletal muscles, hepatocytes, adipose tissues as well as metabolic centers present in hypothalamus 30. A gender specific differential regulation of glucose homeostasis mediated by androgen-AR axis has also been perceived. Androgen deficit in males reportedly leads to altered metabolism and type2 diabetes (T2D), while excess androgen systemically triggers T2D in females 30. Previous work in the lab has elucidated an upregulated expression of AR in the GCs under both in vitro and in vivo PCO conditions (8 and Unpublished Data). Thus, in order to understand the effect of elevated AR levels at the local ovarian levels, considering the crucial function of GCs in providing energy needs of the oocyte, expression of two key glycolytic enzymes GAPDH and PGK1 was analyzed both at the transcript and protein levels. The experiment revealed differential expression of GAPDH and PGK1 in the PCO experimental sets. GAPDH was significantly downregulated while PGK1 was significantly upregulated at both the transcript and protein levels in the PCO set in comparison to the super-ovulated (SO) controls. TQ treatment was able to revert back the condition considerably (Figure 5.1). This observation signifies impaired glycolysis under PCO condition. As the expression of GAPDH is downregulated, affecting energy harness during folliculogenesis; suggested upregulation in PGK1 may imply a compensatory mechanism against the same.

Figure 5.1: Differential expression of glycolytic enzymes GAPDH and PGK1 under PCO condition.

(A) Significant downregulation of GAPDH and upregulation of PGK1 was observed at the transcript level upon performing qRT-PCR. (B) Immunoblotting with whole cell lysates for both GAPDH and PGK1 along with loading control β-Actin confirmed the significantly downregulated expression of GAPDH under the PCO condition. While as observed at the transcript level, PGK1 expression was markedly upregulated in PCO set compared to SO at

the protein level. TQ treatment was able to restore the levels of both the enzymes similar to that of the SO experimental sets. Band intensities of the respective samples were analyzed though ImageJ and normalized with β-Actin intensities and Students T-test was performed for statistical analysis.

5.2 In silico analysis predicting potential interaction between AR and PGK1:

Recent reports suggest glycolytic enzyme, PGK1 stabilizes AR by interacting with it 17. Elevated AR levels under PCO condition combined with the present observation of increased expression of PGK1 in the GCs under PCO instigated us to examine the binding potential of PGK1 and AR via in silico approaches. PDB files of both the protein and the ligand was downloaded and molecular docking by H-dock software was performed. The best interactive model revealed a docking score of -224.79 between AR and PGK1 protein, which was further visualized by PyMOL. The score indicates a strong potential interaction between the two (Figure 5.2A).

It has been predicted that PGK1 mediated stabilization of AR, a nuclear receptor; can take part in the positive feedback loop leading to augmented transcription of PGK1 11. Thus, using bioinformatic tools, we further embarked upon analysis of any probable binding of AR with the PGK1 promoter. PGK1 promoter sequence was downloaded from EPD database. Utilizing the bioinformatics tool, JASPAR, AR binding site at the PGK1 promoter sequence and its relative binding score was predicted. The analysis revealed relative score of 0.8 between AR and PGK1 promoter sequence predicting possible AR binding to PGK1 promoter; which might signify AR's role in elevating PGK1 expression under PCO condition (Figure 5.2B).

Figure 5.2: Predicted interaction between AR and PGK1 from bioinformatics analysis.

(A) Molecular docking by H-dock software reveal a docking score of -224.79 between AR and PGK1 proteins, indicating strong potential interaction between the two. (B) Predicted sequence of AR and its relative binding score to PGK1 promoter sequence as predicted by JASPAR.

5.3 Augmentation of PGK1 expression upon DHT treatment and reversal upon treatment with AR-blocker enzalutamide in KK-1 cells:

The nuclear receptor, AR gets activated upon binding with its ligand (androgens), dimerizes and gets translocated to the nucleus. To decipher whether AR activation leads to increased expression of PGK1 in GCs, KK-1 cells were treated with the AR ligand dihydrotestosterone (DHT) in one set. In another set KK-1 cells were treated with both DHT as well as the AR blocker, enzalutamide, in order to prove that the augmented expression of PGK1, if any is due to activation of AR. Vehicle treated KK-1 and only enzalutamide treated KK-1 acted as controls for the experiment. The protein samples isolated from these treated sets were further subjected to SDS-PAGE followed by western blotting. Immunoblotting for PGK1 revealed a marked elevated expression of PGK1 upon activation of AR in the DHT treated cells, while DHT and enzalutamide treatment led to reduced expression of PGK1. This signifies that the upregulated expression of PGK1 is specifically due to AR activation, hence upon AR blocker, enzalutamide treatment there is a decline in PGK1 [removed]Figure 5.3).

Figure 5.3: Modulation of PGK1 expression by DHT and AR blocker Enzalutamide.

Expression levels of PGK1 significantly increased upon DHT treatment in KK-1 cells and are reversed upon co-treatment with Enzalutamide, indicating AR activation leads to PGK1 upregulation and confirming androgen-AR mediated regulation of PGK1 in GCs.

MATCHED SOURCES:

Report Generated on **May 27, 2025** by https://www.check-plagiarism.com/ (https://www.check-plagiarism.com/)

Check Plagiarism

PLAGIARISM SCAN REPORT

Date	May 27, 2025
Exclude URL:	NO

Unique Content	**100**	Word Count	967
Plagiarized Content	**0**	Records Found	0

CONTENT CHECKED FOR PLAGIARISM:

5.4 Elevated expression and nuclear localization of AR and PGK1 under PCO condition as evident from immuno-fluorescence analysis:

Taking cues from the in-silico analysis and the above experiment implying PGK1 expression is intensified upon AR activation, it was necessary to substantiate this observation, through investigation of the sub-cellular localization of AR and PGK1 in the experimental sets (SO, PCO and PCO+TQ). Immunofluorescence analysis revealed a distinctively elevated expression of both AR and PGK1, concomitant with our previous immunoblot data in the PCO set. Both the proteins were primarily localized in the nucleus under the PCO condition. Intensified co-localization of AR and PGK1 in the nucleus indicated by enhanced yellow colour was also observed in the KK-1 cells under the PCO condition (Figure 5.4); suggesting a positive correlation between these two factors.

Figure 5.4: Immunofluorescence analysis shows nuclear co-localization of AR and PGK1 in PCO samples. Elevated expression of AR and PGK1 under PCO condition as evident from immuno-fluorescence analysis. Intense yellow staining in cells under PCO condition indicates co-localization of AR and PGK1. The observation implies probable AR and PGK1 binding and functional interaction.

5.5 Significant upregulation of glucose transporter GLUT-4 under PCO condition:

Reports suggest that among all the glucose transporters, GLUT-4 is differentially regulated during IR condition while GLUT-1 is constitutively expressed 13. Thus, in order to check the expression status of GLUT-4 in the GCs under PCO condition, RNA was extracted from all the experimental sets and subsequently processed for cDNA preparation after purity check. Further, semi-quantitative PCR amplification was carried out using gene specific primers for the glucose transporter, GLUT-4 along with β-actin gene as the housekeeping control. The analysis revealed significant upregulation in GLUT-4 expression in PCO model compared to SO model, while significant

yet minor reversal of this condition was observed in pre TQ treated set. The expression of GLUT-4 was significantly lower than that of the PCO sample upon TQ pre-treatment but significantly elevated than that of the SO sample (Figure 5.5A).

Cell lysates from the four experimental sets were further subjected to immunoblot analysis using antibody against GLUT-4, which also revealed a significantly elevated expression of GLUT-4 in PCO sample compared to SO. Markedly significant reversal was also observed upon TQ treatment (Figure 5.5B).

Figure 5.5A & B: GLUT-4 expression is upregulated in PCO samples in comparison to SO samples and this augmentation is reverted back by TQ treatment. (A) Semi-quantitative PCR revealed a highly significant upregulation of insulin resistance associated glucose transporter, GLUT-4 transcripts. (B) Protein expression analysis by immunoblotting demonstrated enhanced GLUT-4 expression under PCO conditions in the KK-1 cells as evidenced from transcript analysis, indicating altered glucose uptake that is consistent with the condition of IR. Reversal of GLUT-4 levels is also evident from both the transcript and protein analysis upon TQ treatment.

Subsequently, immunofluorescence assay was performed to visualize the localization and expression of GLUT-4 in all the four experimental sets. Immunofluorescence analysis demonstrated distinctly increased expression of GLUT-4 in the PCO samples, mostly at the cell membrane (Figure 5.5C). This implies augmented glucose uptake under the influence of IR in PCO condition to compensate for the differential glycolysis.

Figure 5.5C: Subcellular localization of GLUT-4 in the various experimental sets.

Immunofluorescence images show GLUT-4 distribution at cell membrane. PCO samples exhibit intensified GLUT-4 fluorescence, suggesting increased recruitment of GLUT-4 which is reverted to SO levels upon pre-treatment with TQ.

5.6 Enhanced glucose uptake under PCO condition:

The evidence of elevated expression of GLUT-4 at the cell membrane of the GCs under PCO condition, suggesting increased glucose uptake; prompted us to assess the glucose uptake capacities of the experimental groups. With that aim in mind, glucose uptake assay was performed utilizing a fluorescent glucose analogue named 2-NBDG (at a final concentration of 100μM) as per protocol by both florescence microscopy 27 (Figure 5.6) and also fluorescence measurement by plate reader 31 (data not shown). In both the experiments, increased fluorescence was observed under PCO condition implying increased glucose uptake, which is concomitant with the increased GLUT-4 expression in PCO set. The fluorescence observed under the PCO+TQ set was similar to that observed under SO condition. Taken together, this data suggests that elevated GLUT-4 levels fuels heightened amount of glucose uptake by the GCs under PCO condition.

Figure 5.6: Analysis of 2-NBDG uptake in GCs through fluorescence microscopy. 2-NBDG fluorescence intensities indicate significantly increased glucose uptake under PCO conditions in comparison to SO, consistent

with elevated GLUT-4 expression. Pre-treatment with TQ restores similar condition as that seen under SO condition. Scale bar represents 10μm.

Earlier studies demonstrated that an intracellular surge in glucose concentration leads to glucose induced oxidative stress 32 33 with generation of reactive oxygen species (ROS) including nitrogen species 34 33. Interestingly, increased ROS has been previously reported under PCO condition both in vitro 35 as well as in patient samples 36. The elevated ROS levels might be the triggering factor for increased autophagic degradation under PCO condition reported by several studies 8 37. Increased apoptosis has also been reported under raised concentration of glucose inside cells 33 38. Thus, intracellular hyperglycemic condition leading towards apoptosis or autophagic degradation might be responsible for generation of atretic follicles and impaired folliculogenesis, resulting in polycystic ovaries.

6. CONCLUSION

The observations from this study signifies a role of increased expression and nuclear localization of AR in regulating several factors associated with glycolysis under the PCO condition bringing about an impaired glucose uptake leading to impaired folliculogenesis (Figure 6). This might have an impact on the developing ova as the GCs are indispensable for the normal growth and function of the ova. Further the interaction of PGK1 and AR needs to be validated via co-immunoprecipitation, which can provide deeper insights about their functions.

Figure 6: Flowchart describing the mechanism of impaired folliculogenesis and ovulation caused by PGK1 overexpression.

MATCHED SOURCES:

Report Generated on **May 27, 2025** by https://www.check-plagiarism.com/ (https://www.check-plagiarism.com/)